الجمهورية الجزائرية الديمقراطية الشعبية
People's Democratic Republic of Algeria
وزارة التعليم العالي والبحث العلمي
Ministry of Higher Education and Scientific Research
جامعة غرداية
University of Ghardaia
كلية العلوم والتكنولوجيا
Faculty of Science and Technology
قسم الالية والكهرو ميكانيك
Department of Automatics and Electromechanics

MEMORY

For obtaining the master's degree
Domain: Material Sciences
Sector: physics
Specialty: energy physics and renewable energies

Title

Characterization of a Swirled Flow Using Artificial Neural Networks

Publicly defended on 01/06/2024

By
ATTIA Bouchra / BEN OUDA Hadjer

In front of the jury composed of:

Dr. Kamel BOUARAOUR	**Univ Ghardaia**	**President**
Dr. Oum Kalthoum LAGHOUITAR	**Univ Ghardaia**	**Examiner**
Dr. Mohamed ARIF	**Univ Ghardaia**	**Examiner**
Dr. Djemoui LALMI	**Univ Ghardaia**	**supervisor**
Dr. Abdeslam Kifouche	**Univ Ghardaia**	**Co-supervisor**

Academic year: 2023/2024

Thanks

ALLAH is the one who helped us and gave us the strength to reach this day.

The first person we would like to thank is our supervisor, Professor Mr. DJEMOUI Lalmi and Mr. KIFOUCHE Abdeslam, for the guidance, confidence and patience which constituted a considerable contribution without which this work could not have been carried out successfully.

We would also like to thank the members of the Jury for agreeing to examine this work.

We would like to express our sincere thanks to all the teachers who taught us from primary to university levels. Finally, I thank everyone who contributed directly or indirectly to the completion of this work.

.

Dedication

(وَآخِرُ دَعْوَاهُمْ أَنِ الْحَمْدُ لِلَّهِ رَبِّ الْعَالَمِينَ)

I thank God for his help and assistance in completing this research

I would like to dedicate this humble work: to in martyrdom and in gratitude for their dedication and constant support during All my years of study, their endless sacrifices, and their sacrifices Moral relief, they are the ones who made a lot of effort for me Educational and seeing me achieve this goal All this and what cannot be said, my emotions are limitless.

to my dear father and dear mother

To those who are the source of my inspiration and courage, to whom I owe love and gratitude. To who were and still are my support.

my uncle and my dear brothers

To my partner in this research, with whom the college brought me together, you were my best companion.

Benouda Hadjer

Finally, I dedicate this work to my childhood friend and supporter, Ghoufrane***, and to all my family members and friends in study and residence.***

Attia Bouchra

Dedication

(وَآخِرُ دَعْوَاهُمْ أَنِ الْحَمْدُ لِلَّهِ رَبِّ الْعَالَمِينَ)

We did not embark on the beginnings except through His facilitation, we did not reach the end except through His success, and we did not achieve the goals except through His grace. Praise be to God, who enabled us to value this step in our educational journey.

I dedicate my highest expressions of gratitude to the foundation of the house, the distinguished man who spent his life for my happiness, may God prolong his life,

to my dear father.

To my soul, my support, my encourager at all times, I ask God to grant her happiness and contentment,

my dear mother.

To those who were the best helpers, may God protect them and fulfill their wishes,

my dear brothers.

To the one who stood by me during the most intense pressures, my friend in situations, my companion in this research,

Bouchra Attia.

Finally, I would like to thank my family members, friends, and those with whom my study and university residency brought me together.

Benouda Hadjer

Abstract:

Throughout history, humans have strived to enhance transportation and energy efficiency while mitigating environmental damage. The discovery of vortex flow in combustion technology has been pivotal, leading to ongoing research into its properties, especially in terms of the shape of the rotational areas it forms. This study delves into the use of artificial intelligence to predict vortex flow properties. Using experimental data, including descriptive and positional information, as inputs, and horizontal, vertical and kinetic energy as outputs across different locations within the combustion chamber, the model effectively captures the spatial features of the swirl flow field. It accurately predicts the velocity density distribution and vortex center position, which is in good agreement with experimental results. Furthermore, the generated prediction model shows promising accuracy over previous data sets, successfully reconstructing the vortex flow field and making inductive predictions on new data with a certain degree of generalizability. Ultimately, this study underscores the potential for many engineering applications to benefit from the prediction model developed here.

Keywords: Swirl, flow, recirculation zone, neural network, training and prediction.

Résumé :

Tout au long de l'histoire, les êtres humains ont cherché à améliorer l'efficacité des transports et de l'énergie tout en atténuant les dommages environnementaux. La découverte du flux tourbillonnaire dans la technologie de combustion a été cruciale, entraînant des recherches continues sur ses propriétés, notamment en ce qui concerne la forme des zones de rotation qu'elle forme. Cette étude se penche sur l'utilisation de l'intelligence artificielle pour prédire les propriétés du flux tourbillonnaire. En utilisant des données expérimentales, comprenant des informations descriptives et positionnelles en tant qu'entrées, et l'énergie horizontale, verticale et cinétique en tant que sorties à différents emplacements à l'intérieur de la chambre de combustion, le modèle capture efficacement les caractéristiques spatiales du champ de flux tourbillonnaire. Il prédit avec précision la distribution de densité de vélocité et la position du centre du vortex, ce qui est en bonne concordance avec les résultats expérimentaux. De plus, le modèle de prédiction généré montre une précision prometteuse sur les ensembles de données précédents, reconstruisant avec succès le champ de flux tourbillonnaire et effectuant des prédictions inductives sur de nouvelles données avec un

certain degré de généralisabilité. En fin de compte, cette étude souligne le potentiel pour de nombreuses applications en ingénierie de bénéficier du modèle de prédiction développé ici.

Mots clés : Tourbillon, zones de recirculation, réseaux neuronal, apprentissage et prediction.

الملخص:

على مر التاريخ، سعى البشر جاهدين لتعزيز وسائل النقل وكفاءة الطاقة مع تخفيف الأضرار البيئية. لقد كان اكتشاف التدفق الدوامي او الدوامة في تكنولوجيا الاحتراق أمرًا محوريًا، مما أدى إلى البحث المستمر في خصائصه وخاصة من ناحية شكل المناطق الدورانية التي يشكلها. تتعمق هذه الدراسة في استخدام الذكاء الاصطناعي للتنبؤ بخصائص التدفق الدوامي. باستخدام البيانات التجريبية، بما في ذلك المعلومات الوصفية والموضعية، كمدخلات، والطاقة الأفقية والرأسية والحركية كمخرجات عبر مواقع مختلفة داخل غرفة الاحتراق، يلتقط النموذج بشكل فعال السمات المكانية لحقل تدفق الدوامة. إنه يتنبأ بدقة بتوزيع كثافة السرعة وموضع مركز الدوامة، مما يتماشى بشكل جيد مع النتائج التجريبية. علاوة على ذلك، يُظهر نموذج التنبؤ الذي تم إنشاؤه دقة واعدة عبر مجموعات البيانات السابقة، حيث نجح في إعادة بناء مجال تدفق الدوامة وتقديم تنبؤات استقرائية بشأن البيانات الجديدة بدرجة معينة من التعميم. في النهاية، تؤكد هذه الدراسة على إمكانية العديد من التطبيقات الهندسية للاستفادة من نموذج التنبؤ الذي تم تطويره هنا.

كلمات مفتاحية: الدوامة -السريان- مناطق إعادة الدوران - الشبكة العصبية - التدريب والتنبؤ .

Summary

CHAPTER II:

ARTIFICIAL NEURAL NETWORKS

CHAPTER III:

METHODOLOGY

List of figures

List of Table

Abbreviations list	
Abbreviations	**Nomination**
ANN	Artificial Neural Network
AI	Artificial Intelligence
CRZ	Central Recirculation Zone
CNN	Convolutional Neural Network
ERZ	External recirculation zone
FFBPNN	Feed-Forward Back-Propagation Neural Networks
IRZ	internal recirculation zone
ISL	Artificial Neural Network
LES	Large eddy simulation
LSB	Low swirl burner
MLP	Multi-layer perceptron
MSE	Mean Squared Error
ORZ	Outer Recirculation Zone
PVC	Precessing Vortex Core
RBN	Radial Basis Networks
RNN	Recurrent Neural Networks
TLC	Thin-Layer Chromatography
RNN	Recurrent Neural Networks

GENERAL INTRODUCTION

GENERAL INTRODUCTION :

Swirling flows, characterized by the rotational motion of fluid particles around a central axis, manifest in a multitude of engineering and natural systems, exerting profound influence on their performance and behavior. From the efficient mixing in industrial processes to the optimization of combustion in propulsion systems, and from the dynamics of oceanic currents to the dispersion of pollutants in the atmosphere, understanding the intricate behavior and characteristics of swirling flows is paramount for a diverse array of applications. However, traditional methods of analyzing swirling flows have often been constrained by their reliance on empirical correlations derived from limited experimental observations.

The advent of artificial intelligence (AI) heralds a new era in the study of swirling flow phenomena, offering unprecedented opportunities to enhance our understanding and predictive capabilities. By harnessing AI techniques, particularly machine learning algorithms, researchers can unlock hidden patterns and relationships embedded within vast datasets of swirling flow simulations and experimental measurements. This approach transcends the limitations of traditional methods, empowering scientists and engineers to develop predictive models that capture the dynamics of swirling flows with unparalleled accuracy.

This interdisciplinary fusion of fluid dynamics principles with AI methodologies holds immense promise for advancing the characterization of swirling flows. Through the deployment of advanced machine learning algorithms such as neural networks, genetic algorithms, and reinforcement learning, this study endeavors to delve deep into the complexities of swirling flow dynamics. By analyzing intricate flow structures, turbulence characteristics, and vortex dynamics, researchers aim to unravel the underlying mechanisms governing swirling flows across diverse spatial and temporal scales.

The outcomes of this research transcend disciplinary boundaries, with profound implications for fields ranging from aerospace engineering to energy production and environmental science. By gaining deeper insights into swirling flow phenomena through the lens of artificial intelligence, engineers and scientists can revolutionize the design of more efficient and sustainable technologies, optimize fluidic processes, and mitigate environmental impacts.

Moreover, the knowledge derived from this study contributes to the advancement of fundamental fluid dynamics principles, laying the groundwork for future innovations in flow control, turbulence modeling, and renewable energy systems.

In summary, the integration of artificial intelligence into the characterization of swirling flows marks a transformative paradigm shift in fluid dynamics research. By harnessing the computational power and analytical prowess of AI-driven methodologies, researchers stand poised to unlock unprecedented insights into the complexities of fluid motion, driving innovation and progress across a myriad of engineering and scientific domains.

The aim of this study is to utilize one of the artificial intelligence models to predict the characteristics of swirling flow. The research focuses on integrating state and spatial parameters to estimate the axial and radial components of velocity, as well as turbulent kinetic energy. The reliability of the model is assessed using statistical parameters such as the error between predicted and measured values, MSE (Mean Squared Error).

The manuscript consists of four parts: an introduction and three chapters. The first chapter describes swirling flows, their current state in research, and their applications. The second chapter provides a detailed overview of integrating artificial intelligence models, including their definition, characterization, using, and comparison. The third chapter presents the selected material and methods used in our study, along with the results obtained and their interpretation. Finally, the study concludes with a conclusion.

CHAPTER I:

BIBLIOGRAPHIC GENERALITIES OF SWIRLING FLOW

I.1. INTRODUCTION:

In the economic context of the last 20 years, combustion improvement remains an important topic for the scientific community. This improvement has seen the use of high-flow, high-energy burners, to reach high temperatures. It is clear that the fires produced within these installations must necessarily be stable in order to limit any risk an accident occurs. One of the most common ways to achieve this result is to hold the flame in a vortex flow. The latter also makes it possible to optimize the combustion process and reduce polluting emission. The peculiarity of these tortuous flows is their three-dimensional and unstable structure with varying turbulence and Curvature of their current lines. They also contain strongly nonlinear phenomena, the most famous example being vortex explosion (PVC) [1]. In this chapter, we present a bibliographic study on swirl flows and their effect on combustion efficiency.

I.2. SWIRLED FLOWS:

We say that a flow is "rotating" when the fluid has rotational motion relative to the main direction of flow. Turbulent vortex flows are used in many industrial applications. For non-interactive flows, we can cite hurricane separators, jet eddies or agricultural sawmills. For reaction flows we can cite piston engines and some industrial furnaces. Natural phenomena such as tornadoes. In recent years, vortex flows have been commonly used in combustion processes in order to achieve flame stability [2]. The problem of flame stabilization is the main criterion in the design of combustion chambers. Applications using very low flow speeds, of the order of laminar flame speed or lower, present natural stability. As for applications with higher flow speeds (most industrial applications, especially in the context of aviation) [3], flame stabilization is done through different strategies to ensure stability, the most important of which are:

- Self-ignition:

The phenomenon of self-ignition was common in the high compression ratio spark ignition engine. Such as diesel engines, where the air is heated by pressure before fuel is injected. This mechanism is also mainly used in the case of supersonic combustion (jet aircraft). The air flow is at a very high temperature due to the high-pressure levels. When the

auto ignition process occurs, the reactants are hot enough to ensure that combustion begins despite the rapid entry of the reactants [3].

- The Continuous maintenance of a heat source:

Continuous ignition can be ensured by a secondary flow of hot gas, an external heat source (electric for example), or even a secondary pilot flame. The flame by Sandia D [4], shown in Figure.1, is an example of a non-premixed flame stabilized by a premixed pilot flame.

Figure.I.1: Photograph of the so-called Sandia D flame. The central jet (25% methane and 75% air in volume) is surrounded by 72 poor pilot flames (mixture of C2H2, H2, air, CO2 and N2) **[5]**

-Creating a recirculation zone:

In a region where the flow velocity and flame propagation speed are the same magnitude, the flame can stabilize due to the slowdown of the flow. In addition, the recirculation zone allows burned gases from the combustor to be returned to the flame, several solutions are possible to force recirculation:

- The first consists of introducing an obstacle (“bluff body”) or a sudden widening of the passage section to promote the formation of recirculation zones.
- Another possibility is to rotate the flow. The rotation of the fluid on itself causes a depression in the axis. If this drop is large enough, it can create recirculation on the tube

axis when the jet opens into the chamber at the level of sudden expansion. The rotation causes the jet to expand and form a central recirculation zone favorable for flame stabilization. This second solution is often preferred in the aviation context because it results in lower pressure losses, and installation takes place away from walls [6]. It also makes it possible to improve the mixing rate by increasing the turbulent activity in the burner, to stabilize the flame and to design more compact devices. The flame of flying burners is therefore often stabilized by the rotational motion of the reagents entering the chamber surrounding the burner axis (vortex) imposed by the injector geometry [3].

I.3. GENERALITY OF SWIRL:

I.3.1. Effect of swirl:

The swirl makes it possible to add a tangential component of the velocity field to a flow. This results in a balance between the centrifugal forces acting on the fluid particles and the pressure forces in a confined flow, giving the flow a curvature effect at the level of the mixing zone. The swirl makes the structures coherent, strongly organized in the case of the jet free, weaker by removing vortex-pairing (pairing of vortices) and by promoting an increase in turbulence (Panda and McLaughlin [7]). It was observed that from certain swirl intensity (i.e. an azimuthal component in the high velocity field) a recirculation zone appeared in the main flow.The size and position of this recirculation zone vary with the intensity of the swirl (Beér and Chigier [8], Leuckel and Fricker [9], Escudier and Keller [10], Sheen et al. [11]). This zone is an essential element for stabilizing combustion because it contains fresh preheated gases and allows the flame to hold.

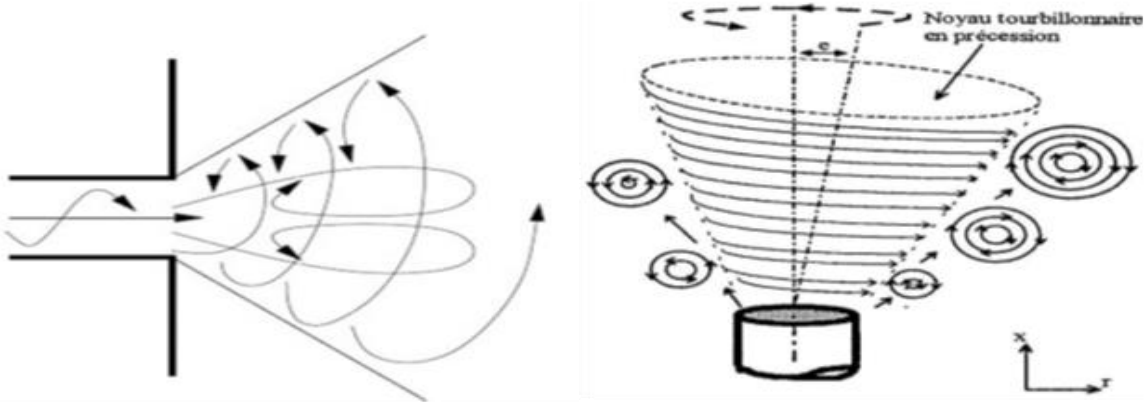

Figure.I.2: Diagram describing the swirl effect **[12]**

I.3.3. Effect of swirl on combustion:

Above all, to stabilize a flame, it is necessary to have a permanent and sufficiently intense heat source in order to initiate combustion reactions. For this, aerodynamic devices are used in industry. Which is intended to create a lower burner nose, recirculation zone [12]. It is the last, it is the best way to obtain a good mixture. The very good mixing induced by the swirl results in a reduction in the size of the flame [13]. The length in length is also due to a reduction in supply of oxygen in the upper part of the flame downstream of the IRZ [14] and the increase in the reaction rate [15]. The swirl affects the evolution of the length of the flame as a function of the wealth. Thus the increase in richness does not modify the length of the flame for jet flames, but leads to a linear increase in the length of the flame with a swirl. The IRZ created by the swirl constitutes a thermal source which traps the products combustion and constitutes hot spots at the heart of the reactive flow. This reserve of combustion products allows better stabilization of the flame. It then becomes possible to significantly reduce the poor extinction limit.

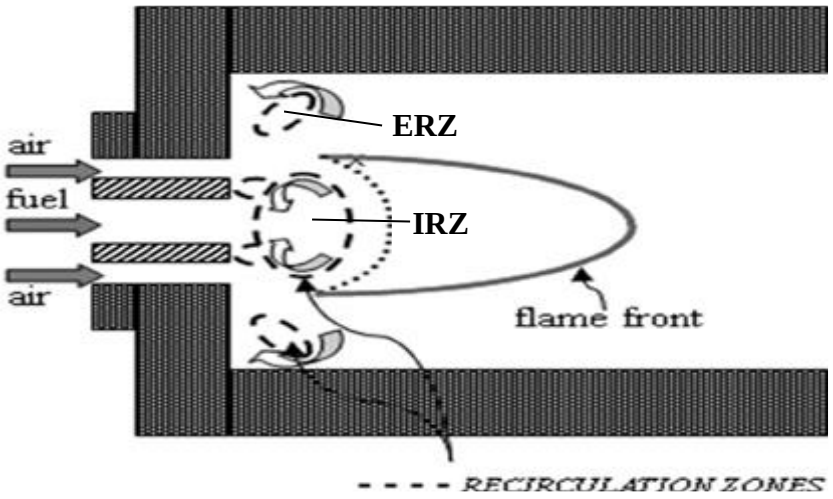

Figure.I.3 : Internal external recirculation zones **[16]**

I.3.4. Effect of swirl on pollution:

The effect of the swirl varies depending on the situation, it increases or reduces NOx [15]. Schmidt et al. [17] showed that the use of swirl in unmixed combustion can lead to reduced pollutant emissions, especially NOx emissions. In fact, under the effect of swirl and thus

improving the mixing of reactants, the flame temperature decreases and leads to a decrease in the production of NOx. In addition, hypoxia reduces the formation of emission pollutants, and conversely, excess oxygen tends to increase those pollutants (increase When the vortex intensity is sufficient), increasing the number of vortices leads to a decrease in the residence time, which is the main parameter governing the formation of NOx. Flame size and temperature are also reasons for the increase of NOx. However, in all cases, the effect of the swirl on pollutant emission levels is positive because it allows for a reduction in wealth and thus a reduction in NOx [18].

I.3.5. Number of swirls:

Rotating flows are characterized by a dimensionless number: the swirl number denoted S_n A consensus exists to define the swirl number as being the ratio of the axial flux of tangential momentum $G_g$to the product of the radius of the pipe by the axial flux of axial momentum G_x.

$$S_n = \frac{G_w}{R\, G_x} \qquad \text{(I.1)}$$

$\boldsymbol{G_w}$: represents the tangential momentum flow.

$\boldsymbol{G_x}$: represents the axial momentum flow.

R: is the characteristic radius of the flow.

This number allows us to describe the intensity of the flow rotation. The higher this number, the stronger the swirl. The fluxes $\boldsymbol{G_g}$ and $\boldsymbol{G_x}$ are given by the following expressions **[29].**

$$\boldsymbol{G_w} = \int_0^R \rho u_g u_x 2\pi r^2\, dr \qquad \text{(I.2)}$$

$$\boldsymbol{G_x} = \int_0^R (\rho u_x^2 + P) 2\pi r\ dr \qquad \text{(I.3)}$$

According to equations (I.1) and (I.2), (I.3) we find

$$S_n = \frac{\int_0^R \rho u_w u_x 2\pi r^2\, dr}{\int_0^R (\rho u_x^2 + P) 2\pi r\ dr} \qquad \text{(I.4)}$$

$\boldsymbol{u_g}$**:** Tangential of speed.

$\boldsymbol{u_x}$**:** Their respective components axial.

$\boldsymbol{P}$**:** The static pressure of the column.

If the pressure term is negligible then:

$$S_n = \frac{2\pi \int_0^R \rho u_g u_x r^2 \, dr}{2\pi \int_0^R (\rho u_x^2 r \, dr} \qquad \text{(I.5)}$$

To designate the experimental value of Swirl number, one must have access to the u_x and u_g components of the velocity field and pressure (P) on the cross sections of the rotating flow. The recirculation zones are present, in the regions where the value of the "Critical Swirl", S_n= 0.6.

I.3.5.1. Influence of the number of Swirl on the flame:

Chen and Driscoll [19] showed that when the number of swirls increases, the length of the flame can be reduced by a factor of 5. The swirled flow therefore makes it possible to obtain more powerful flames while being more compact. In comparison with a standard burner, a swirl burner therefore makes it possible to reduce the size of the installation due to the compactness of the flame produced. Chen [20] also noticed that the formation of NOx, which is a pollutant, depends on the number of swirls. Through his experiments, he was able to show that the higher the number of swirls, the more the formation of NOx decreases.

Susset [21] for his part highlights that increasing the number of swirls makes it possible to obtain a more stable flame. He explains that the lower the number of swirls, the more the flame appears "soft" and moves chaotically. To prove this result, he has everything simply compared two flames with a respective swirl number of S=0.1 and S=0.82. He observed that for the lower number of swirls, the reactive zone is wider and its position fluctuates more radially than for a higher number of swirl.

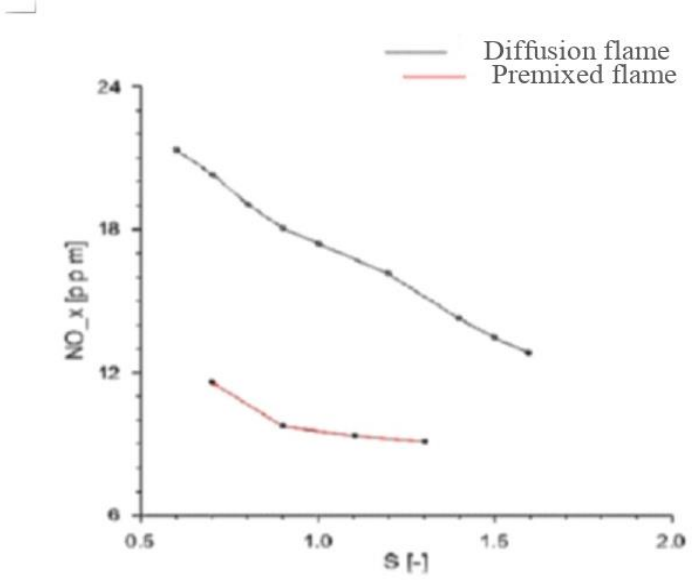

Figure.I.4: Effect of swirl number on NOx production **[22]**

I.3.6. The effect of swirl on a flow:

I.3.6.1. Non-reactive flow:

Because of the effect of the number of swirl on the flow. Make swirls flows divided into two categories: low vortex flows (S_n < 0.6) and high vortex flows (S_n > 0.6).

I.3.6.1.1. Weakly Swirled Flows (S_n < 0.6):

For flows with a low number of swirls, no recirculation zone appears. The swirl induces an increase in the entrainment of the ambient fluid at rest and a decrease in the axial speed of the flow. The velocity profiles of a weakly swirled flow remain Gaussian until approximately S_n<0.6. The degree of opening of the jet as well as the flow of entrained mass then increases continuously with the number of swirls. [9].

I.3.6.1.2. Strongly Swirled Flows (S_n > 0.6):

For a swirl intensity of approximately 0.6, a recirculation zone appeared in the main flow. The size and position of this recirculation zone vary with the swirl intensity [9]. This zone is an essential element for stabilizing the flames because it contains fresh preheated gases and allows for better combustion One of the important characteristics of this recirculation zone is that its center approaches the nose of the nozzle (or injector) and that its size increases as the number of swirls of the flow increases.

I.3.6.2. A reactive flow:

Beér and Chigier [8] explain the effect of swirl intensity on flame behavior as shown in the figure:

- Type A (S_n < 0.6) flame: The swirl intensity is low (low S_n), and the flame behavior is similar to that encountered without swirl. The flame front is located at a certain distance from the burner. An external recirculation zone (ORZ) is formed around the main jet, and the flame is separated from the burner.

- Type B flame (0.6 < S_n < 1.3): The intensity of the swirl is moderate or moderate, and the recirculation zone and flame stabilization appear near the burner. This type of combustion is generally required, due to the presence of high turbulence and intense combustion levels in the recirculation zone rich in fresh gas.

- Type C flame (S_n > 1.3): The swirl intensity is high (high S_n), the interactions between the flame and the walls are intense. This is an undesirable condition in general, except in the case of certain ovens. With regard to diffuse combustion (in the case of central injection of Fuel injection and external annular oxidation injection.) And imagine that the oxidants are recycled sufficiently to stimulate the recycling zone.

Leuckel and Fricker [9] highlight two types of flame:

- The speed of the fuel is high enough to pass through the entire zone, only a small part of the fuel burns as it passes through the recirculation zone and is then used in the pilot flame for the installation: the remaining fuel is preheated. The flame is therefore intense and long.
- The speed of the fuel is not sufficient, it spreads radially. The mixture is rapid and the flame becomes short and blue.

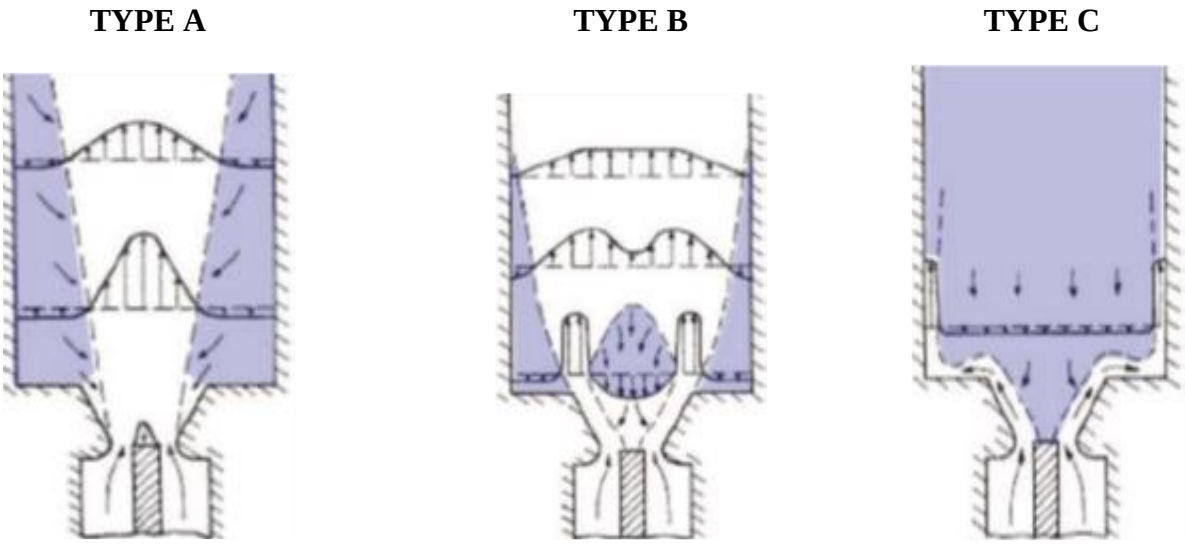

Figure.I.5: Flow topology for different swirl levels. Areas in blue materialize the recirculation zones induced by the swirl **[15]**

In a multistage injection system consisting of an axial swirl and a radial inlet. The figure shows the flow topology at the outlet of this type of injector, that is, it shows the flow and the main vortex structures identified at the burner outlet. There are fluid shear zones between the recirculation zones and the main flow: The ISL (Inner Shear Layer) designates the shear zone between the ORZ (Outer Recirculation Zone) and the main flow. These shear zones are characterized by significant speed levels [23].

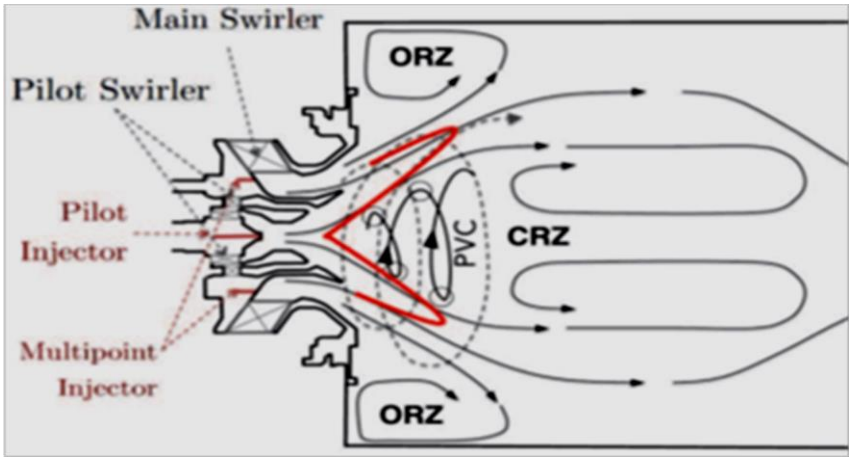

Figure.I.6: Diagram of the main vertical structures identified at the exit of the system TLC injection [**23]**

I.3.2. Swirl generation techniques:

There are several ways to generate the rotation of a flow. They can be classified into three main categories:

- Use of fins or adjustable propellers tangentially deflecting the axial flow. Because of its simplicity, this device is generally used in industrial systems [24,25]. The intensity of the vortex is limited (depending on the design of the fins) [26]. It directly depends on the angle formed by the fins with the longitudinal direction. More precisely, the number of vortices is directly proportional to the tangent of this angle (Beér and Chigier [8]) whatever the Reynolds number Re of the flow, except for very low values of this number ($Re \geq 600$) where the corrective limit function of Re.
- Rotating mechanical devices which generate a rotational movement to the fluid passing between them [27].
- Rotation of a tube [28] or a plate [29]. However, the swirl generated is very weak. This type of device is rather intended for the study of swirl breakdown, which is an example of the recirculation region of swirled flows and is one of the Rotation Tube representations [30].
- Accidental injection of part or all of a fluid into a main conduit. The swirl intensity is then determined by the ratio between tangentially injected and axially injected flow [31, 32].

I.4. THE TECHNOLOGICAL ADVANTAGES OF SWIRL STABILIZATION:

Turbulent swirling flows provide multiple advantages in flame stabilization:

- Swirl clamping is more commonly used compared to flame spark clamping, because it is done using a pneumatic stop. It therefore makes it possible to overcome the thermos mechanical limitations associated with the presence of mechanical parts in the reaction zone where the gases are the hottest.
- The swirl motion contributes to increased mixing efficiency of the reagents, resulting in reduced NOx and facilitating flame stabilization.
- The swirl feature is flame compression that reduces flame slackness, and since combustion occurs in a smaller volume, this allows for reducing the size of the burner.

The stable flame at the front of the central recirculation zone is called "V" or "M," due to its distinctive Figure (I.7, I.8) [33].

- Another very important feature of the recirculation zone is that it allows it to play the role of an energy tank between the combustion detectors, so the large amount of gas contained in the recirculation zone makes it possible to stabilize the flame over a wide range of operation. On the other hand, the velocity gradients are interesting in the shear zone located between the recirculation zones and the main plane.

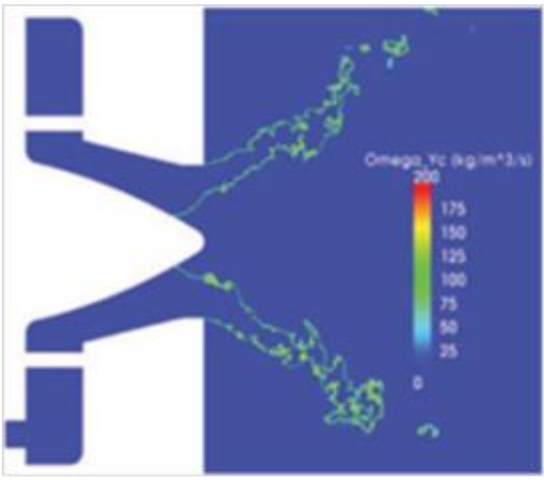

Figure.I.7: Shaped flame in the PRECCINSTA materialized by the advancement variable**.** in the median plane (Moureau et al **[34]**).

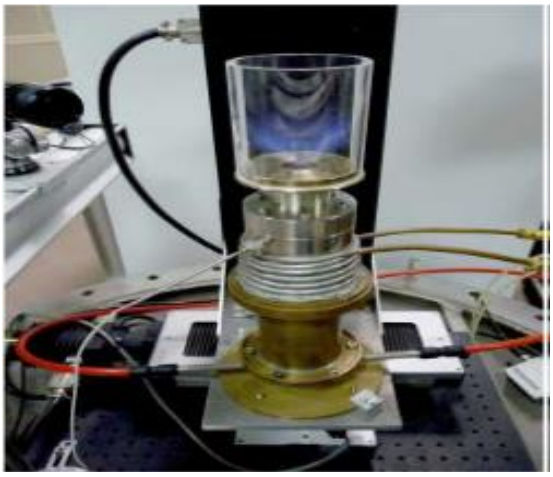

Figure.I.8: Visualization of the laboratory flame studied in Palies' thesis **[33].**

I.5. BIBLIOGRAPHIC STUDY (STATE OF THE ART):

Leuckel [35] (1967) proposed a vortex technique with moving blades in order to vary the vortex intensity. In fact, the same moving blade technology was used in the **TECFLAM** burner [27] (2000). Therefore, the choice of vortex type is crucial for ZRI formation and flame stabilization.

In order to reduce nitrogen oxide (NO_x) emissions in industrial combustion systems, the use of injectors operating in lean and pre-mixed combustion systems has become widespread in recent years. but, in this system, strong combustion instabilities can occur and damage the device or cause the flame to go out. An overview of recent studies on combustion in vortex flows was given by **Syred and Beer** (1974) [36], In (1981) more recent studies were

conducted by **Claypole, N. Syred** on combustion chambers with vortex flows. These studies focus on the effect of vortex levels on aerodynamics and NOx emissions at constant load [37]. Studies on the vortex effect, on the limits of flame stability were performed in (1981) by **Rawe and Kremer** [38], flame stabilization by **Hillemanns, Lenze** in (1988) [39], and flame explosion limits (flame blowing) in (1990) by **Driscoll** and **al** [40].

In (1992), the LSB technology was invented by **Chan C.K**. It is a technology that focuses on low vortex burners [41]. The flame is stabilized by the weak vortex generated by the air injectors. Continuing the previous LSB development efforts, additional testing was conducted in 1995 by **R.K.Cheng** and **B. Bédat** developed a methodology for studying turbulent flames that were previously stabilized by a low number of vortices. Most importantly, their results were the starting point for many studies on flame stabilization and pollutant reduction (NOx) methods, and the low vortex burner (LSB) was an essential part of the development of the technology [42].

In 1996, researchers conducted experimental investigations aimed at establishing a new correlation for the eddy number concerning a radial-type vortex generator under various Reynolds numbers and vane angle settings. They employed a radial-type vortex generator equipped with 16 rotating guide vanes to produce a rotating annular jet flow, covering Reynolds numbers ranging from 60 to 6000 and vane angles from 0° to 56°. Under low Reynolds number conditions, **H.J. Sheen, S.Y. Jeng**, and their colleagues observed a strong correlation between vortex strength, Reynolds number, and guide vane configuration. Utilizing the experimental findings, they developed a modified vortex number, denoted as S, to characterize the vortex flow, facilitating improved vortex generator design [43]. In 1997, **Zhang and Nieh** conducted numerical and experimental investigations on turbulent vortex flow and combustion of pulverized coal within a novel vortex combustor (VC), employing the algebraic Reynolds turbulence model (ARSM). They provided detailed insights into flow and combustion dynamics, encompassing turbulence, temperature, species concentrations, particle densities, trajectories, combustion time, and residence time [44]. By 2000, their research revealed the formation of a recirculation zone within the VC when gas flowed through a central coaxial tube with multiple air injections. They also noted that swirl effectively regulated the gas molecule sliding speed within the VC [45].

In 2005, **Ying Huang** and **Vigor Yang** conducted a numerical investigation on the impact of inlet swirl on flow development and combustion dynamics in a lean-premixed swirl-stabilized combustor. They utilized a large-eddy simulation (LES) technique coupled with a level-set flamelet library approach. Their study yielded findings regarding the influence of augmenting the number of vortices on the recirculation area, as well as enhancing turbulence intensity and flame speed [46].

Khelil and **al**. [47] (2009) dealt with the numerical prediction of a highly swirling natural gas diffusion flame in a confined environment. The numerical calculation was carried out by the commercial code Fluent. The RSM turbulence model uses to describe turbulent flow. The PDF probability density function (β function) model (9 species and 8 reactions) with a chemical equilibrium model is used to model the turbulence-chemistry interaction. Their main objective is to determine polluting emissions and to numerically study the factors that influence the combustion process by comparing the results with experimental measurements.

In (2010) **Yilmaz** and **al** carried out a study of the effect of adding hydrogen to a burner low number of swirl by examining the behavior of the flame and its stability. The results show that the combustion characteristics are very sensitive to the hydrogen fraction in the combustible mixture improving flame stability [48].

Brahim Sarh et al. [49] (2014) Are interested in the study of experimental characterization of a swirled, non-premixed turbulent flame of oxygen-enriched methane-air, with the aim of experimentally characterize the effects of global parameters, such as the O2 content in the oxidant, the overall richness at injection and the swirl intensity on the stability of the flame, polluting emissions and the dynamic behavior of the reactive flow.

In (2016). **Ouali** et **al** carried out a numerical simulation of pre-mixed flames turbulent suspended methane/air stabilized by swirl for a burner configuration LSB with a 50 mm diameter nozzle for two configurations, 2D and 3D where the effect of Methane richness (Φ from 0.6 to 1.4) was studied for both. While the effect of the number of swirl (S from 0.5 to 1.0) was studied only in 3D configuration. They used the model RANS k-ε STANDARD for modeling turbulence and two models for combustion modeling, EDM (Eddy Dissipation Model) and Partially-Premixed. [50] The interest of their studies is the optimization of

temperature and the number of swirls while ensuring stability with minimum NOx and CO emissions. **Elbaz** and **Roberts** [51] (2016) made detailed measurements of the turbulent flow

field, gas species concentrations and temperature field in a swirling flame of unpremixed methane. Particular attention is paid to the effect of geometry (straight quarl and converging quarl) on flame structure and emission characteristics due to its importance in gas turbine and industrial burner applications. They found that the structure of the main flame is controlled by the rotation of the swirled air flow, the straight quarl geometry, the turbulence pattern, mixing fraction, temperature distribution, emissions and stability of the flame. Gives the internal recirculation zone (IRZ) a rapid and complete mixing which reduces the residence time of NO formation. The prediction of a set of detailed and complete chemical reactions in the annular combustion chamber of a gas turbine with 18 burners, and on the other hand, an annular combustion chamber consisting of 16 identical premixed swirled burners were simulated with the Large Eddy Simulation (LES) model [52, 53].

Industrial needs force researchers to find new solutions Simulation tools and design techniques to access various Engineering configurations. **Li Gang** et **al**. [54] (2017) Testing the new design for a new injector with rotating lobes at different angles (Figure I.13). Lobed vortex injector can play an effective role in generating vortex and improving mixing. In addition, by adjusting the axial position of the vortex lobes, unmixed combustion can develop into premixed combustion, and vice versa, tested in low eddy burner configuration.

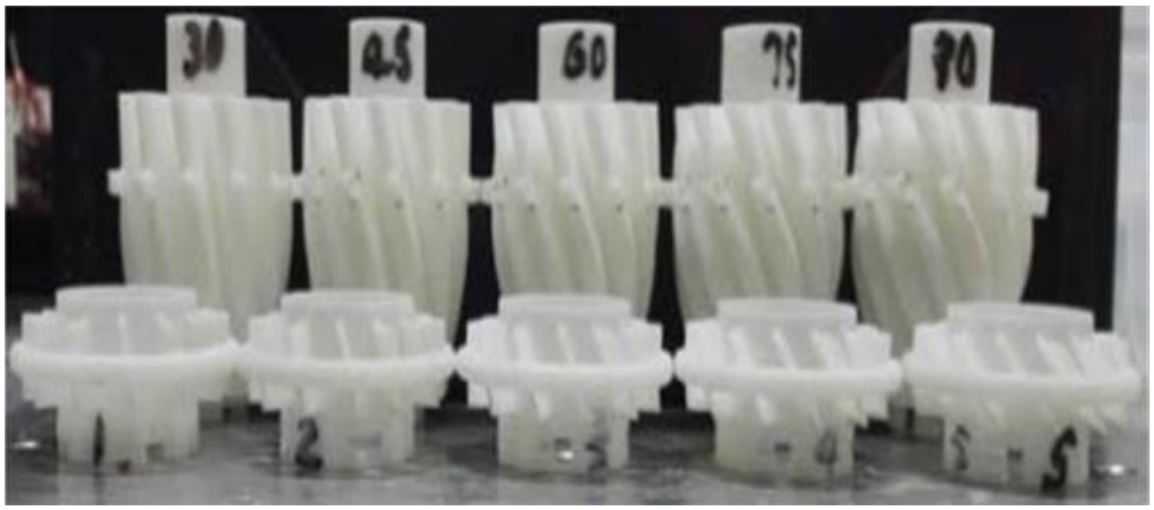

Figure.I.9: Photos of swirled and vortex lobate configurations with different inclination angles **[54]**

In (2022) **Mohamed ELBAYOUMI** numerically studied the effect of adding hydrogen to methane and the intensity of turbulent swirl flow, under lean and stoichiometric mixing conditions. A wide hydrogen addition ranges (up to 90%) is used for different swirl intensity levels. The results demonstrate that adding hydrogen to methane appears to offer a viable solution towards a carbon-free fuel [55].

In 2023, **Junqing Zhang**, **Chunjie Sui**, and others conducted a comprehensive large eddy simulation using OpenFOAM to examine the impact of vortex intensity on combustion characteristics in vortex-ally stabilized ammonia/methane combustion. The study's numerical findings were validated through experimentation. Results indicate that swirl intensity significantly influences the flow field and flame structure, with flame stability decreasing as swirl intensity rises. Higher swirl intensity leads to flame extinction at the root, while lower swirl intensity fails to create the central recirculation zone necessary for flame stabilization. Selective non-catalytic reduction (SNCR) of NO emerges as crucial for NO emission control, with temperature reduction promoting NO reduction, while reduced residence time inhibits NO reduction. Furthermore, SNCR weakens the correlation between NO and OH in ammonia/methane combustion [56].

In this research (2024), a swirling combustion furnace was designed and manufactured to achieve lean combustion. The effects of several factors, such as swirling air ratio, equivalence ratio, and thermal power, on the lean combustion process were studied. The results showed that the combustion chamber temperature rises when the swirling air ratio is 100%, and the emissions of nitrogen oxides (NOx) and carbon monoxide (CO) are at their lowest in this condition. Additionally, an appropriate equivalence ratio increases the combustion chamber temperature while reducing NOx and CO emissions during lean combustion. It was also found that carbon dioxide (CO2) emissions reach a minimum at a specific thermal power, while temperature and NOx emissions increase with thermal power. The research indicates high stability of the lean combustion process under all experimental conditions, demonstrating the potential of the swirling combustion furnace to achieve clean and efficient combustion [57].

CONCLUSION:

In this chapter we were able to obtain a bibliographic study on vortex flow. We initially mentioned the importance of vortex flow in the combustion community, its role in enhancing flame stability, and its common use in efficient fuel-air mixing. One of the main properties of vortex jets is the creation of recirculation zones, especially in the center of the room. These zones capture burning gases and have low velocities where the flame can "cling." We then discussed the effect of vortex on the flame structure as well as on the formation of pollutants, especially nitrogen oxides. We also discussed the concept of the eddy number and its effects, which is a dimensionless number that allows these flows to be described, and we refer to it as S.

CHAPTER II:

ARTIFICIAL NEURAL NETWORKS

II.1. INTRODUCTION:

Artificial neural networks (ANN) mimic the computational structure of biological neural systems, which include interconnected neurons. These neurons communicate via weighted links, enabling signal transmission. The process includes data collection, analysis, network design, simulation, and testing. Artificial neural networks find applications in various fields, facilitating data processing, analysis, prediction and identification of new data in areas such as speech recognition, imaging, control and optimization, among others. It has real-life applications in finance, medicine, business, mining, etc… [58]. Initially inspired by biological systems, artificial neural networks evolved from simplified neuronal models developed by McCulloch and Bates in 1943 [59].

In this chapter we introduce the basic concepts for understanding artificial neural network and describe the relationship between biological and artificial NN.

II.2. BIOLOGICAL NEURONS:

The human body comprises a diverse range of living cells, some of which are interconnected to facilitate communication of pain or activation of fibers or tissue [60]. This activity involves the transmission of electrical triggers from one neuron to another along the neuron's axon, facilitated by an electrochemical process of voltage-gated ion exchange [61].

While each neuron independently executes a simple task, like responding to an input signal, the true power of neural networks emerges when these neurons are interconnected. Together, they can tackle intricate tasks like speech and image recognition swiftly and accurately [62]. A neuron typically comprises dendrites, a cell body, and an axon, as illustrated in Figure. II.01:

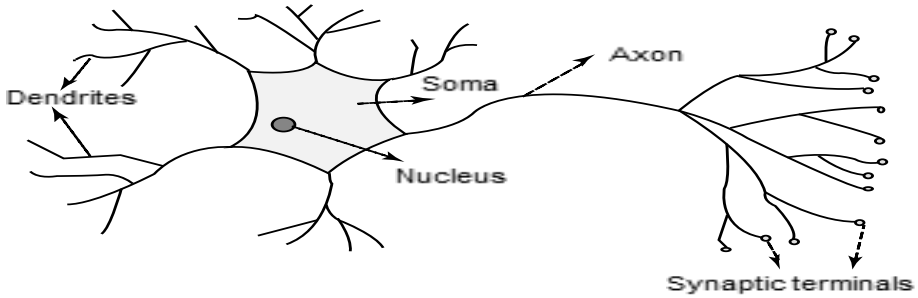

Figure.II.1: Biological Neuron **[59]**

-Dendrites: The dendrites are branched structures connected to the cell body, extending to receive signals from other neurons in space [62].

-cell Body (Soma): The cell body, also called the soma, contains the nucleus [62], is where most of the neural "computation" takes place [61].

-axon: is the transmitter of the neuron. it sends signals to neighboring neurons [62].

-Synapses: The connection between the end of one neuron's axon and the neighboring neutron's dendrites is called the synapse, which is the communication unit between two neurons [62].

Electrochemical signals propagate across the synapse. If the cumulative signal received by a neuron exceeds the synapse threshold, it triggers the neuron to fire, sending an electrochemical signal to adjacent neurons [62].

II.3. ARTIFICIAL NEURON:

An artificial neuron serves as the fundamental unit within artificial neural networks, mirroring the structure and functions observed in biological neurons, which are the building blocks of biological neural networks such as the brain, spinal cord, and peripheral ganglia.

Comparisons in design and functionalities are illustrated in Fig.3, wherein the left side depicts a biological neuron with its soma, dendrites, and axon, while the right side portrays an artificial neuron with its inputs, weights, transfer function, bias, and outputs [63].

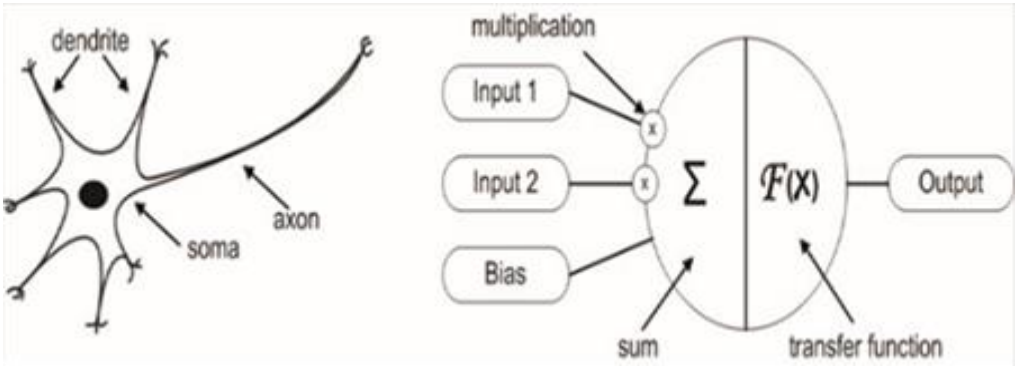

Figure.II.02: Biological and artificial neuron design **[63].**

The artificial neural network consists of four sections:

- (layer input) X_i:

Inputs are directly the inputs to the system or can come from other neurons. It is symbolized by (X_1, X_2…X_n).

-Bias:

Are the inputs which are always set to 1 and which allow flexibility to be added to the network by varying the triggering threshold of the bias weight during learning.

-Weights:

Weights are the multiplying factors which affect the influence of each input on the exit from the neuron.

-Output layer:

The output of the neural network can be distributed to other neurons [64].

In the context of a biological neuron, data is received through dendrites, processed within the soma, and transmitted via the axon. Conversely, within an artificial neuron, information enters the neuron's body through weighted inputs, where each input is multiplied by a specific weight. The neuron's body then combines these weighted inputs with a bias and processes the sum using a transfer function. Finally, the artificial neuron delivers the processed information through its output(s). The advantage of the artificial neuron model lies in its mathematical simplicity, as demonstrated in the description below:

$$y(k) = F(\sum_{i=0}^{m} w_i(k).x_i(k) + b) \qquad \text{(II. 1)}$$

Where:

$\mathbf{x}_i(\mathbf{k})$: is input value in discrete time k where i goes 0 from to m

$\mathbf{w}_i(\mathbf{k})$: is weight value in discrete time k where i goes 0 from to m.

b : is bias.

F: is a transfer function.

$\mathbf{y}(\mathbf{k})$: is output value in discrete time k [63].

II.3.1. Activation functions:

These functions relate to processing the data received by the neural units [65]. Activation functions, also known as threshold functions or transfer functions [66], play a vital role in artificial neural networks by facilitating learning through non-linear mappings between input and output data. While linear activation functions exist, non-linear ones, such as the sigmoid, tanh, and rectified linear unit (ReLU) [67], are more commonly used as they enable the network to capture non-linear relationships inherent in most real-world data. This capability allows the network to learn complex dependencies that cannot be adequately represented by linear functions [68].

II.3.1.1. Types of Neural Networks Activation Functions:

-Linear function:

it is a function whose output image is similar to the input and provides unlimited multiple classifications ;(artificial neurons perform a simple linear transformation on the sum) .Its formula is: $F(x) = ax$ [69].

-Binary step function:

is a binary function that contains only two possible output values (such as zero and one). The output value becomes equal to one if the input value meets a certain threshold. and if specific threshold is not meet that results in different output value, According to the following formula [70]:

$$y = \begin{cases} 1 & if\ w_i x_i \geq threshold \\ 0 & if\ w_i x_i < threshold \end{cases} \qquad \text{(II. 2)}$$

-Non-linear Function:

Non-linear activation functions solve the limitations and drawbacks of simpler activation functions, such as the vanishing gradient problem. Non-linear functions, such as Sigmoid, Tanh, Rectified Linear Unit (ReLU), and numerous others.

There are several advantages to using non-linear activation functions, as they can facilitate back propagation. Non-linear combinations and functions used throughout a network

mean that data scientists and machine learning teams creating and training a model can adjust weights and biases, and outputs are represented as a functional computation.

In other words, everything going into, though, and out of a neural network can be measured more effectively when non-linear activation functions are used, and therefore, the equations are adjusted until the right outputs are achieved [70].

- **SIGMOID FUNCTION:** The sigmoid function is extensively employed as an activation function due to its nonlinear nature. This function transforms values into the range of 0 to1. Mathematically, it can be expressed as follows:

$$F(x) = \frac{1}{e^{-\mu x}} \qquad \text{(II.3)}$$

Sigmoid function is continuously differentiable and a smooth S-shaped function. The derivative of the function is:

$$f'(x) = [1 - Sigmoid\ (x)] \qquad \text{(II.4)}$$

x: the product of multiplying the input value with its weight.

$\boldsymbol{\mu}$: represents the slope of the function and is equal to 1.

And its derivative:

$$f'(x) = F(x)[1 - F(x)] \qquad \text{(II.5)}$$

- **TANH FUNCTION:**

This function is the Hyperbolic Tangent function, often denoted as Tanh. Similar to the sigmoid function, Tanh is symmetric around the origin, resulting in outputs from previous layers with different signs, which are then passed as input to the next layer. Mathematically, it can be defined as:

$$f(x) = 2sigmoid(2x) - 1 \qquad \text{(II.6)}$$

Tanh is continuous and differentiable, with values ranging from -1 to 1. Unlike the sigmoid function, Tanh has a steeper gradient. It is preferred over the sigmoid function because its gradients are not limited to a specific direction and it is zero-centered.

- **RELU FUNCTION:**

ReLU (Rectified Linear Unit) is a popular non-linear activation function extensively used in neural networks. Unlike other functions, ReLU ensures that not all neurons are activated simultaneously, meaning a neuron is only deactivated when the output of its linear transformation is zero. Mathematically, it's defined as:

$$f(x) = max\,(0, x) \qquad \text{(II.7)}$$

This characteristic makes ReLU more efficient, as only a certain number of neurons are activated at any given time. However, in some cases, the gradient value can be zero, leading to weights and biases not being updated during the backpropagation step in neural network training [71].

II.3.1.2. The role of the need for the activation function:

Neural networks are comprised of layers of neurons, with nodes responsible for classifying and predicting data based on input. These networks typically include an input layer, one or more hidden layers, and an output layer. Each layer contains nodes, and every node has a weight that influences the flow of information between layers.

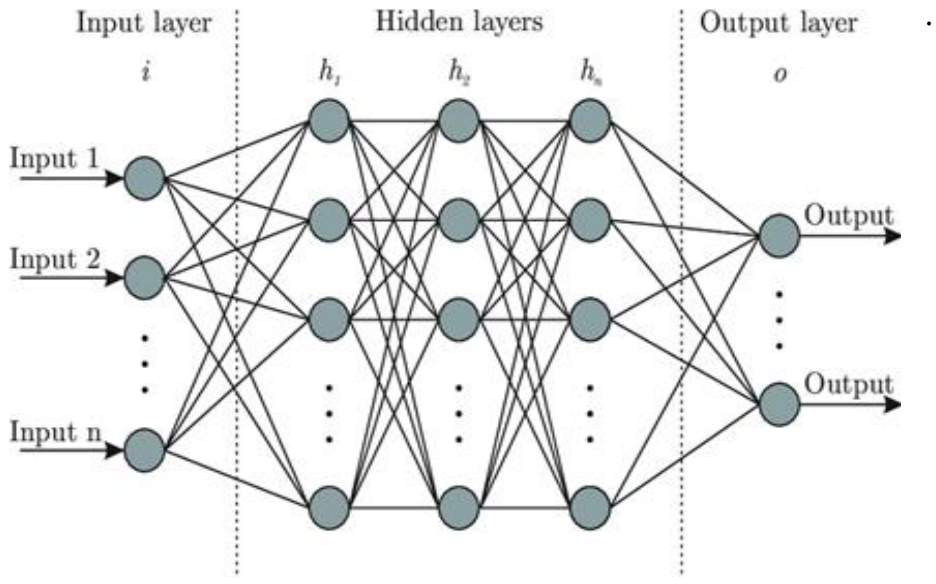

Figure.II.03: Neural Network **[71]**

Without an activation function in a neural network, the output signal would be a simple linear function, akin to a polynomial of degree one. While linear equations are straightforward, their ability to handle complex data mappings is limited. Essentially, a neural network lacking an activation function behaves like a Linear Regression Model, often with restricted performance capabilities. To tackle intricate tasks such as modeling images, videos, audio, speech, or text, it's essential for neural networks to employ activation functions and techniques like Deep Learning. These methods enable the model to make sense of complex, high-dimensional, and nonlinear datasets by incorporating multiple hidden layers [71].

II.4. TYPE OF ARTIFICIAL NEURAL NETWORKS:

Various neural network architectures cater to different types of data and applications. Each architecture is tailored to excel in specific domains or data types, ranging from the fundamental to the intricate. Let's begin with the basic models and progress towards the more sophisticated ones.

II.4.1. Perceptron:

The Perceptron stands as the simplest and earliest version of neural networks. Comprising a single neuron, it processes inputs by applying an activation function to generate a binary output. Lacking hidden layers, it's limited to binary classification tasks. The neuron conducts input processing through weighted summation, followed by activation function application for binary output generation [71].

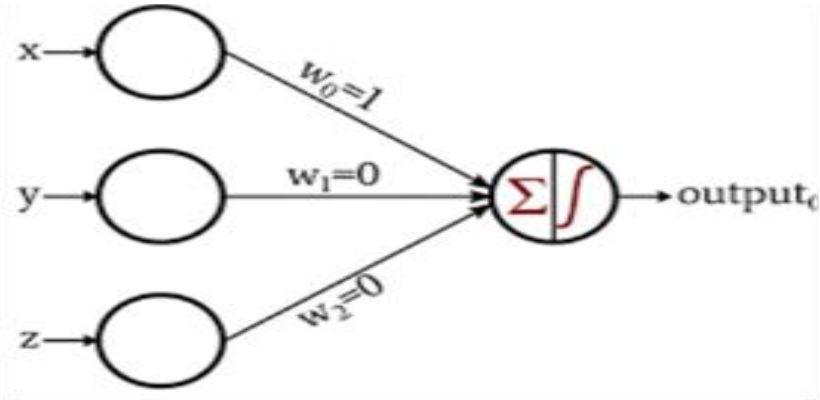

Figure II.04: Perceptron Simple **[73]**

II.4.2. Feed forward network FF:

A neural network that follows a feed-forward topology is known as a Feed-Forward artificial neural network. This architecture mandates unidirectional data flow from input to output without any feedback loops. It imposes no restrictions on the number of layers, types of transfer functions per neuron, or inter-neuron connections. The simplest form of a feed-forward artificial neural network is a single-layer perceptron [63].

FF networks are used in:

- Classification.
- Speech recognition.
- Face recognition.
- Pattern recognition [72].

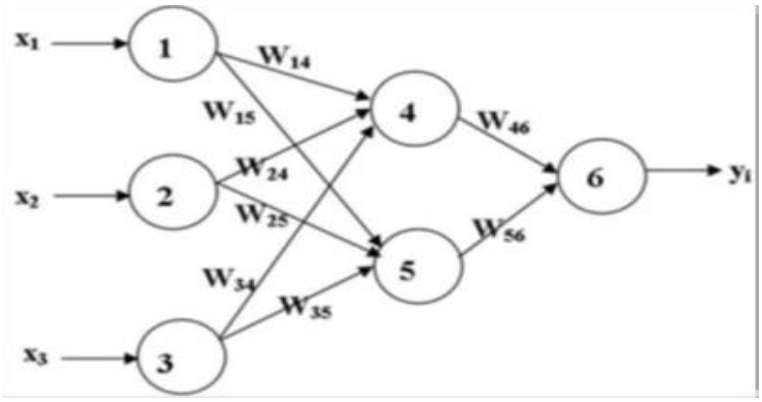

Figure.II.5: An Example of a feed-forward neural network **[73]**

II.4.3 Multi-layer perceptron MLP :

The primary limitation of Feed Forward networks was their inability to learn through backpropagation. Multi-layer Perceptrons (MLPs) address this by incorporating multiple hidden layers and activation functions. Learning occurs in a supervised manner, updating weights via Gradient Descent. MLPs facilitate bidirectional learning: forward propagation of inputs and backward propagation of weight updates. Activation functions vary based on the target type; SoftMax for multi-class classification, Sigmoid for binary classification, etc. Often termed dense networks, all neurons in a layer connect to those in the next. While prevalent in Deep Learning applications, they tend to be slow due to their intricate structure[72].

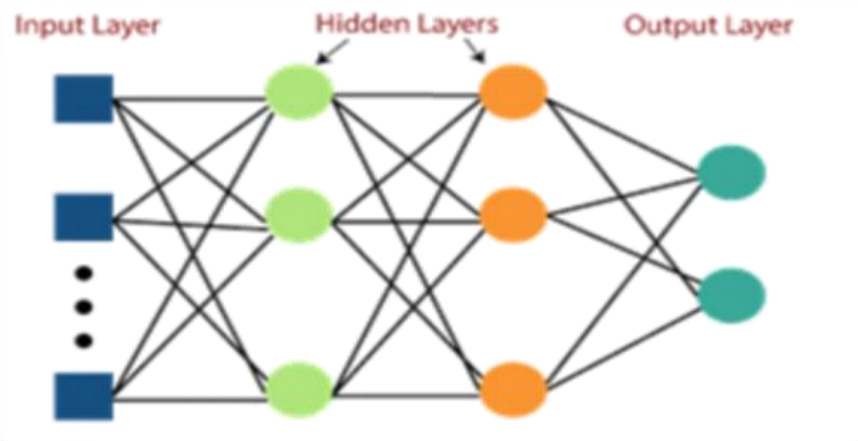

Figure. II. 6 : Multi-Layer Perceptron (MLP) **[73]**

II.4.4. Radial basis networks:

Radial Basis Networks (RBN) utilize a unique approach to predict targets. They consist of an input layer, a layer with Radial Basis Function (RBF) neurons, and an output layer. Unlike traditional Multilayer Perceptrons, RBNs employ the Radial Function as an activation function.

When new data is inputted into the network, RBF neurons measure the Euclidean distance between the feature values and the actual classes stored in the neurons. This process resembles identifying the cluster to which a particular instance belongs. The predicted class is assigned based on the minimum distance. RBNs find extensive application in function approximation tasks such as Power Restoration systems [72].

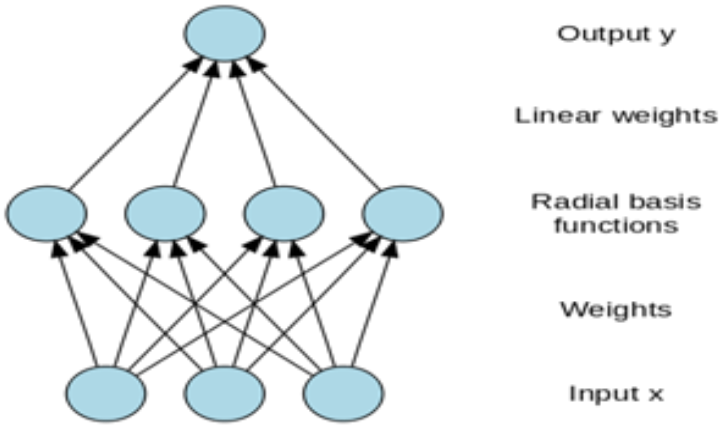

Figure II.07: Radial Basis Networks **[73]**

II.4.5. Convolutional neural networks:

A convolutional neural network (CNN) is designed to process input stored in arrays, commonly used with 2D arrays like images or spectrograms of audio. While they excel in handling 3D arrays like videos, their application to 1D arrays such as signals is growing.

The architecture of a CNN typically comprises three main layers: convolutional layers, pooling layers, and a classification layer. Convolutional layers serve as the backbone, where weights define a convolution kernel applied to the input. The output is then passed through a non-linearity, often ReLU, enhancing the network's capability to capture complex patterns.

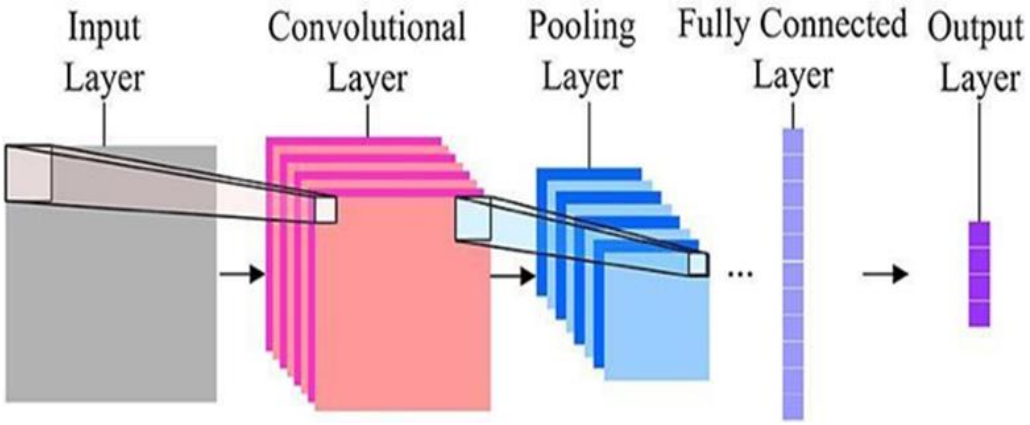

Figure.II.8: convolutional neural network (CNN) **[75]**

CNNs have a wide range of applications, with notable success in computer vision tasks like scene and object detection, as well as object identification. Their versatility extends across fields from biology to facial recognition [74].

II.4.6. Recurrent neural networks:

An artificial neural network with a recurrent topology is referred to as a recurrent artificial neural network (RNN). Unlike feed-forward neural networks, RNNs have no restrictions on back loops, allowing information to be transmitted both forward and backward to form directed cycles [63]. RNNs excel in handling sequential data, making them well-suited for time-dependent tasks. These networks leverage their internal memory to process input sequences of any length [75]. The diagram in Figure II.09 illustrates a compact fully recurrent artificial neural network, showcasing the intricate interconnections among its artificial neurons.

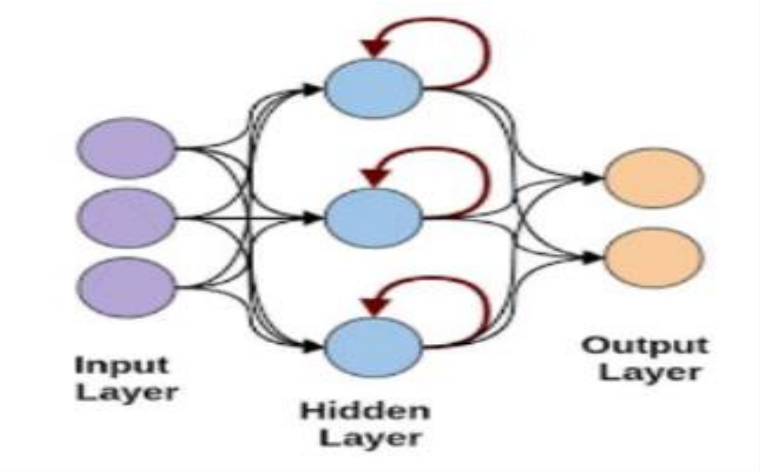

Figure. II.09: Recurrent artificial neural **[72]**

II.5. AREAS OF APPLICATION OF ARTIFICIAL NEURAL NETWORKS:

Today, artificial neural networks find myriad applications across various sectors:

- Processing: including character and signature recognition, image compression, shape recognition, image encryption, classification, and more.
- Signal processing: encompassing filtering, classification, source identification, speech processing, etc.
- Control: spanning process control, diagnosis, quality control, robot control, and beyond.
- Optimization: covering planning, resource allocation, management, finances, etc.
- Simulation: involving model replication, prediction, and more [76].

Moreover, modern applications of artificial neural networks extend to studying swirling flow properties, applying them to photovoltaic fault detection and diagnosis [77], and leveraging artificial nerve cells for high-performance calculations to enhance the transportation of energy sources [78].

II.6. ADVANTAGE OF ARTIFICIAL NEURAL NETWORKS:

- **Storing information on the entire network:** Unlike traditional programming, where data is stored in a database, in artificial neural networks (ANNs), information is distributed throughout the network. Thus, the loss of certain pieces of information in one area does not hinder the network's functionality.

- **Working with incomplete knowledge:** Trained ANNs have the ability to produce output even when provided with incomplete data. The extent of performance degradation in such cases depends on the significance of the missing information.
- **Fault tolerance:** Even if one or more cells within an ANN are corrupted, it can still generate output, showcasing its fault-tolerant nature.
- **Machine learning capability:** ANN learn from past events and are capable of making decisions based on similar occurrences.
- **Parallel processing capability:** ANN possess the ability to execute multiple tasks simultaneously due to their parallel processing capabilities [79].

II.7. DISADVANTAGES OF ARTIFICIAL NEURAL NETWORKS:

- **Hardware dependence:** Artificial neural networks rely on processors with parallel processing capabilities, aligning with their architecture. Consequently, their implementation is contingent upon hardware availability.

- **Unexplained behavior of the network:** This remains a significant challenge for ANNs. While they provide solutions, they often lack transparency regarding the reasoning behind their decisions, undermining trust in the network.

- **Determination of proper network structure:** Establishing the optimal structure for artificial neural networks lacks a definitive guideline. Achieving an appropriate network structure typically entails iterative processes based on experience and trial and error. [79].

CONCLUSION:

In this chapter, we were able to study the concepts of artificial neural networks and shed light on their relationship to biological neural networks. We mentioned the role of the activation function in work artificial NN and its most important functions, and the modern applications of artificial neural networks in various research and their benefits, a brief summary of their types, we have succeeded in providing readers with all the prior knowledge they need to move for.

CHAPTER III:

METHODOLOGY

III.1. INTRODUCTION:

Many industrial processes leverage vortex flows to enhance combustion efficiency. The vortex flow field, generated by the head vortex, crucially impacts fuel and air mixing uniformity, thus influencing temperature distribution at the combustion outlet and facilitating the formation of internal recirculation zones for high volumetric heat release rates and flame stability.

By introducing swirling air through concentric rings, additional control over flow and vortex distribution is achieved, leading to diverse combustion characteristics such as varying flow patterns, turbulence levels, and flame stability limits. Therefore, obtaining a clear understanding of the vortex flow field's characteristics is pivotal for combustion design.

To research the fields of vortex flow and study its characteristics, use one of the artificial neural network models, which focuses on integrating state parameters and spatial parameters to estimate the axial and radial components of the velocity, in addition to turbulent kinetic energy, and compare the expected and measured values by measuring the error rate (R, R^2, MSE) to evaluate the reliability of the model.

III.2. EXPERIMENTAL SYSTEM AND RESEARCH METHOD (DATA COLLECTION):

III.2.1. Generic Model Combustor:

The experiments were carried out using an atmospheric air blast atomizer in a cylindrical combustion chamber [80]. The atomizer consists of a modular arrangement of two radial swirl generators, an atomizer lip which separates the two airstreams from each other within the nozzle, and an air diffuser with a throat diameter of $D_0=2R_0=25$ mm.

For both airflows a constant air preheats temperature of $T_0= 50$ °C has been selected. The mass flow rate of air is adjusted to 64 kg/h ($M_i/M_0=0.37$). Theoretical swirl numbers S_0, the of the inner as well as the outer airflow are $S_i=0.46$ and $S_0=1$, resulting in global swirl number of 0.81. The Reynolds number is calculated as the product of the axial average air velocity at the nozzle exit (39.9 m/s) and the throat diameter of the diffuser divided by the kinematic viscosity of the air and yields approximately 60 000.

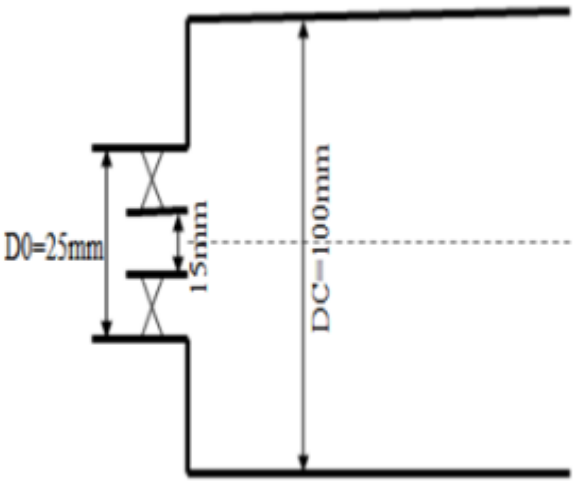

Figure. III.1: Generic Model Combustor.

Measurements of the position and state parameters of the vortex flow field inside the combustion chamber were made using a sensor. Record the experimental values in a table.

Include data:

- Column 1: Height h.
- Column 2: Radius R.
- Column 3: Axial velocity u.
- Column 4: Radial velocity v.
- Column 5: Tangential velocity w.
- Column 6: Kinetic energy k.

III.3. PROPOSED FEED FORWARD BACK PROPAGATION NETWORK (FFBPN) APPROACH:

There are several factors that can be considered for model development that have a greater impact on the vortex flow state (recirculation zones). The proposed methodology began by collecting a dataset from a general model of combustion. Six parameters were determined, and these samples were taken as input to the FFEBN model to extract vortex flow field characteristics. The FFBPN technique was used to train the performance model from

two-way iterations. The first method involves calculating the forward step of the input weights and the second method is calculating the reverse step to update the weights and calculate the errors. Seventy percent of the collected data was used to train the model, while 30% of the data was divided equally for testing, 15% for validation. The overall methodology is presented in Figure.III.2:

Secondly, the model was trained based on Equation (III.1) to generate more accurate output values:

$$y(k) = F(\sum_{i=1}^{m} w_i . x_i + b) \qquad \text{(III.1)}$$

Where $y(k)$ is the new value of the variable, x_i is the initial value of the variable and is the value of the connection weight of the neuron, and b is bias. The activation function between the input and the hidden layer was "SIGMOID", as shown in Equation (III.2).

$$F(x) = \frac{1}{e^{-\mu x}} \qquad \text{(III.2)}$$

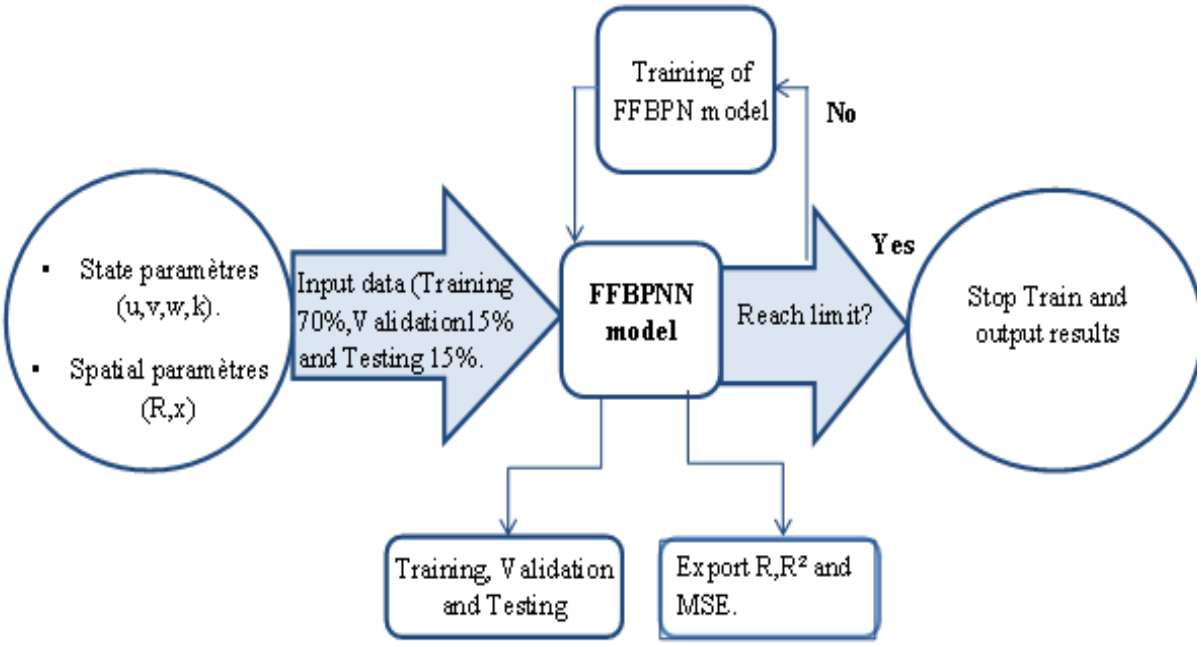

Figure.III.2: FFBPN approach workflow.

III.3.1. Development of the FFBPN model:

The FFBPN model was developed using **MATLAB**. In the initial training phase, the model is trained with the available data. If the model fails to meet expectations, it allows the weight and bias updating process to be continuously redeployed and improved until it reaches the best requirements using the Levenberg-Marquardt (LM) back propagation algorithm [81]. After completing the model training, 15% of the data was used to validate the trained model in the validation phase. The model was also allowed to go through the testing phase and tested with the remaining 15% of the data sets, and the results are accurate when the R^2 value approaches 1. This network consists of three layers, i.e. the input layer, the hidden layers, and the output layer.

-Input layer: The input layer consists of a group of neurons whose number is equal to the number of inputs that we will rely on and we will take as inputs the axial velocity u, radial velocity v, tangential velocity w, radius R, length h and kinetic energy k. If the goal is to predict

the axial velocity u, the input is (R.h.v.w.k), but if the goal is to predict the radial velocity v, The input is (R.h.u.w.k). As for the kinetic energy K, the input (R.h.u.v.w). The neural network learns the characteristics of the input data for later use in the prediction process, so the number of neurons in the input layer will be 5.

-Hidden layer: The hidden layer consists of a group of hidden layers, and their number is determined according to the type of study and the number of inputs, and their number is often small, so in this model we will rely on ten (10) hidden layers, but as for the number of hidden neurons, it is variable.

-Output layer: Since the goal of the study is to predict the axial velocity u, radial velocity v, or kinetic energy k in the vortex flow, the output layer consists of a single neuron.

Thus, the structure of the neural network used will be as shown in the figure.III.3:

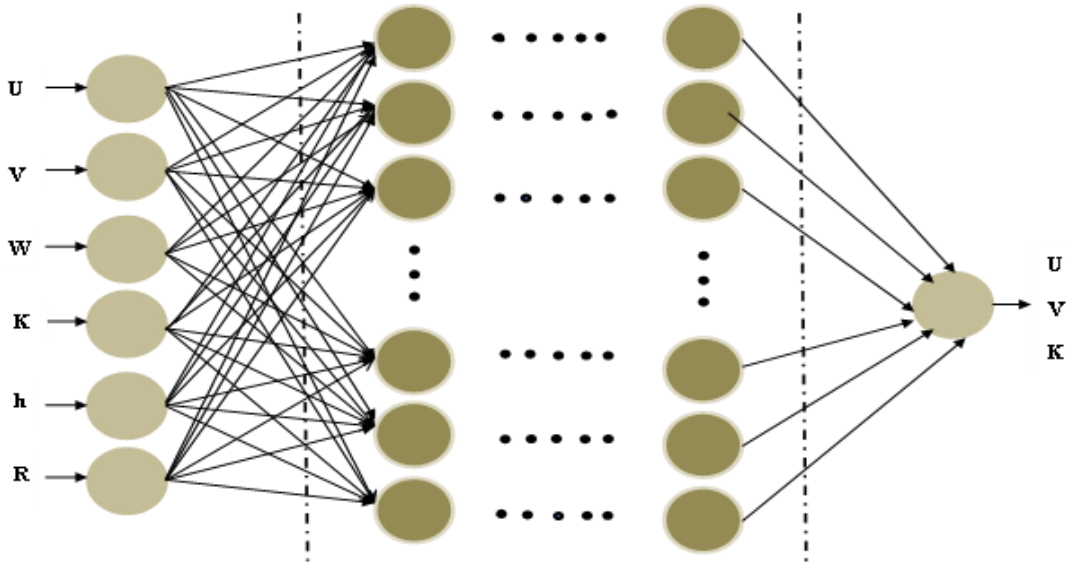

Figure.III.3: The structure of the neural network.

III.4. RESULTS AND DISCUSSIONS:

III.4.1. FFBPN Model Training, validation and testing:

In this study, we aim to establish the FFBPNN framework for predicting eddy flow fields. This involves comparing and analyzing prediction accuracy, goodness of fit, and training costs across models with varying numbers of hidden neurons to identify the optimal configuration.

A FFBPN neural network is developed to accurately predict the axial velocity (u), radial velocity (v), and kinetic energy (k) of vortex flow. Given the limited data availability, specific factors were selected as inputs for model development. The model was trained using equation (1) and the Levenberg-Marquardt backpropagation algorithm, then validated and tested across various datasets. Mean Squared Error (MSE) is utilized to quantify the error between FFBPN-predicted values and experimental data. The goodness of fit is assessed quantitatively using the coefficient of determination (R^2), where a higher R^2 value within the range [0, 1] indicates better fitting. The expressions for R^2 and MSE are as follows:

$$R^2 = 1 - \frac{\sum_{i=1}^{n}(y_{inp} - y_{otp})^2}{\sum_{i=1}^{n}(y_{inp} - \bar{y}_{inp})^2} \quad \text{(III.3)}$$

$$MSE = \frac{1}{n}\sum_{i=1}^{n}(y_{inp} - y_{otp}) \quad \text{(III.4)}$$

The overall R^2 and overall MSE values changed mostly as the number of hidden neurons varied, ranging from a minimum of 14 to a maximum of 28, as shown in Table.III.1:

Number of Neurons	Axial velocity u		Radial velocity v		Kinetic energy k	
	MSE	**R^2**	**MSE**	**R^2**	**MSE**	**R^2**
14	7.11×10^{-4}	0.99701	4.824×10^{-4}	0.99576	1.6×10^{-3}	0.99535
15	10^{-3}	0.99562	1.2×10^{-3}	0.98975	1.139×10^{-4}	0.93471
16	8.124×10^{-4}	0.99659	6.435×10^{-4}	0.99437	1.5×10^{-3}	0.99472
17	9.116×10^{-4}	0.99622	4.224×10^{-4}	0.99626	1.32×10^{-4}	0.97223
18	1.7×10^{-3}	0.99327	7.119×10^{-4}	0.99371	6.976×10^{-4}	0.98474
19	5.894×10^{-4}	0.99752	2.494×10^{-4}	0.99779	3.706×10^{-4}	0.97914
20	1.3×10^{-3}	0.99432	9.113×10^{-4}	0.99199	5.1534×10^{-4}	0.98672
21	9.715×10^{-4}	0.99593	3.571×10^{-4}	0.99686	3.208×10^{-4}	0.99429
22	**9.024×10^{-4}**	0.9962	3.891×10^{-4}	0.99658	1.377×10^{-4}	0.98943
23	**3.364×10^{-4}**	**0.99858**	2.925×10^{-4}	0.99742	2.545×10^{-4}	0.95825
24	1.1×10^{-3}	0.9553	5.136×10^{-4}	0.99546	9.907×10^{-4}	0.97994
25	9.5×10^{-4}	0.99614	5.696×10^{-4}	0.99494	4.816×10^{-4}	**0.99617**
26	2×10^{-3}	0.99151	**2.461×10^{-4}**	**0.99785**	**9.365×10^{-5}**	0.9269
27	2.6×10^{-3}	0.98974	5.791×10^{-4}	0.99487	1.8×10^{-3}	0.9893
28	4×10^{-3}	0.984	4.845×10^{-4}	0.99573	2.582×10^{-4}	

Table.III.1: overall R^2 and MSE values versus number of hidden neurons**.**

It has been found that the accuracy of the developed model is very sensitive to the number Hidden neurons. From Table.III.2 the best network structure was found to be [5× 23× 1] for the network predicts of the axial velocity u, but for the network predicts v or k, the best structure is [5 × 26× 1]. R^2 and MSE values along typical ANN phases with variation in hidden neurons are depicted in Figure (III.4, III.5 and III.6). The error must be continuously evaluated in each state of the neural network to choose the optimal network architecture.

Defining an error function - conventionally referred to as a loss function - is essential for this purpose. It can be used to calculate the model loss, allowing the weights to be updated to minimize the loss of the next evaluation.

It is worth noting that all stages have R^2 values close to 1.0 and MSE values close to 0, with 23 and 26 hidden neurons shown in Figure 4 and 5,6 respectively by the dotted line.

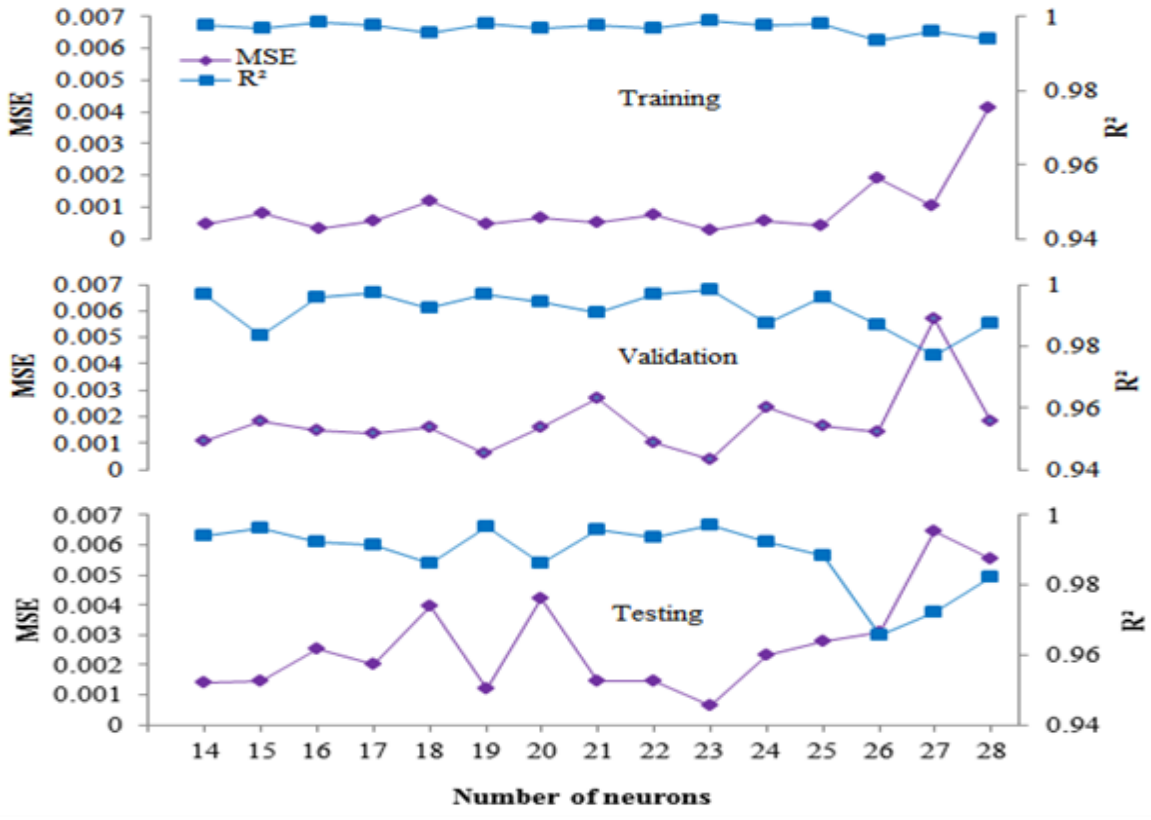

Figure.III.4: Variations in MSE and R^2 values with number of neurons, for axial velocity u.

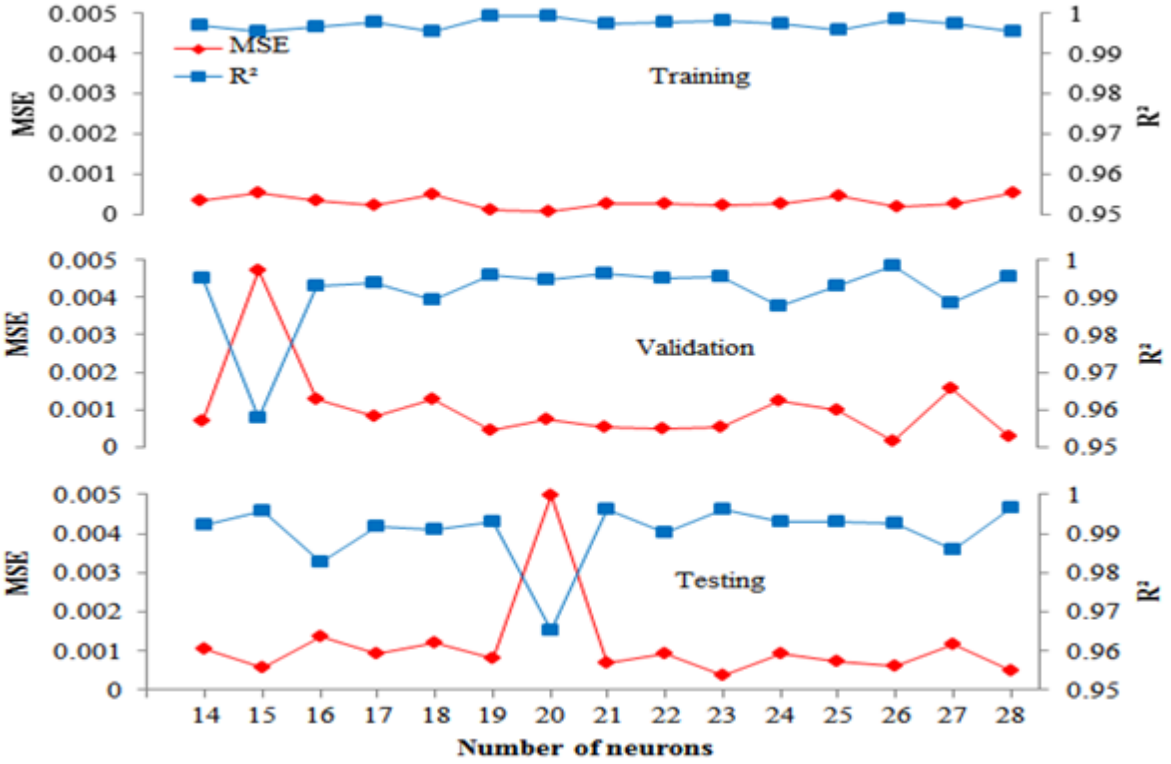

Figure III.5: Variations in MSE and R^2 values with number of neurons for radial velocity v.

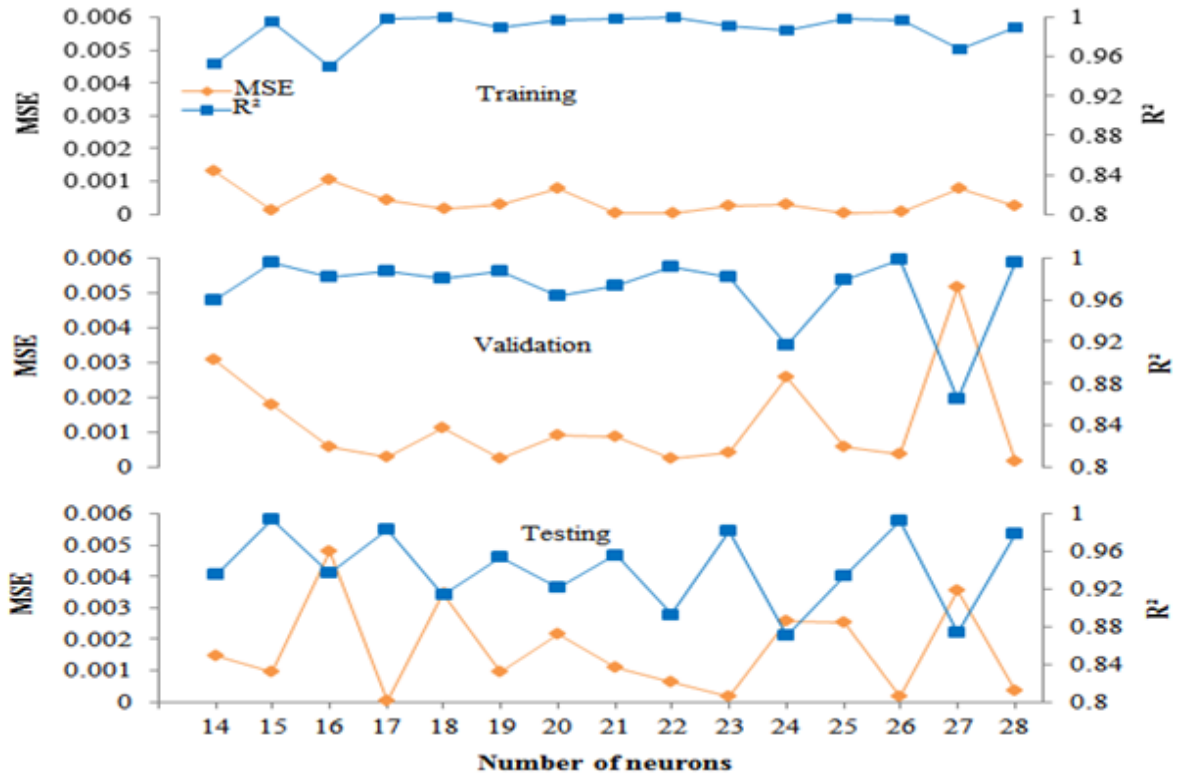

Figure.III.6: Variations in MSE and R^2 values with number of neurons for Kinetic energy k.

III.4.2. FFBPN Model prediction:

Model training is carried out based on the ANN framework constructed above, and then a DNN model with high accuracy is obtained to predict the flow field distribution.
Figure (III.7, III.8, III.9) represents a comparison between the ANN predicted values and experimental data for axial velocity u, radial velocity v, and kinetic energy k for the training set (70 %), the validation set (15%), and the test set (15%) of the datasets. That is, it represents a summary of the R^2 plots at the training, testing, and validation stages during the training process. An overall R^2 value of 0.9998 was obtained for the axial velocity u, 0.99785 for the radial velocity, and 0.99617 for the kinetic energy k. Which indicates that the results are satisfactory, because the overall R^2 score is close to 1.

It can be seen that the R^2 for the training, testing and validation phase has high values in the range (0.992 - 0.999). That is, the data points are basically distributed around the line y = x, with some values deviating from the straight line, that is, the data points are basically distributed around the line y = x, with some values deviating from the straight line despite the existence of a relationship between experimental and expected, while maintaining a certain degree of linear correlation and the ability of the model to reflect the main properties of the vortex flow field, i.e. goodness of fit. Between the expected and experimental values of u, v, and k are high.

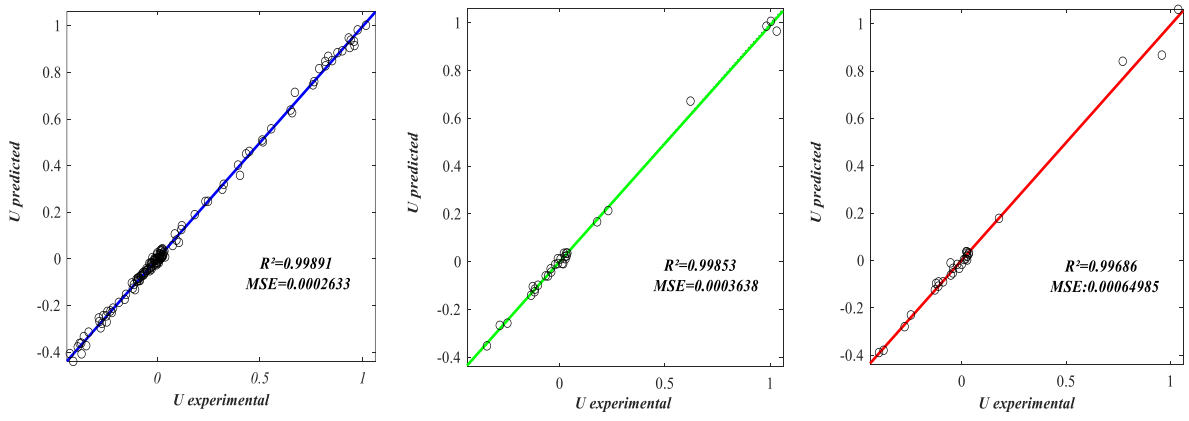

Training set *Validation set* *Testing set*

Figure.III.7: Regression. Axial velocity u in training, validation and testing

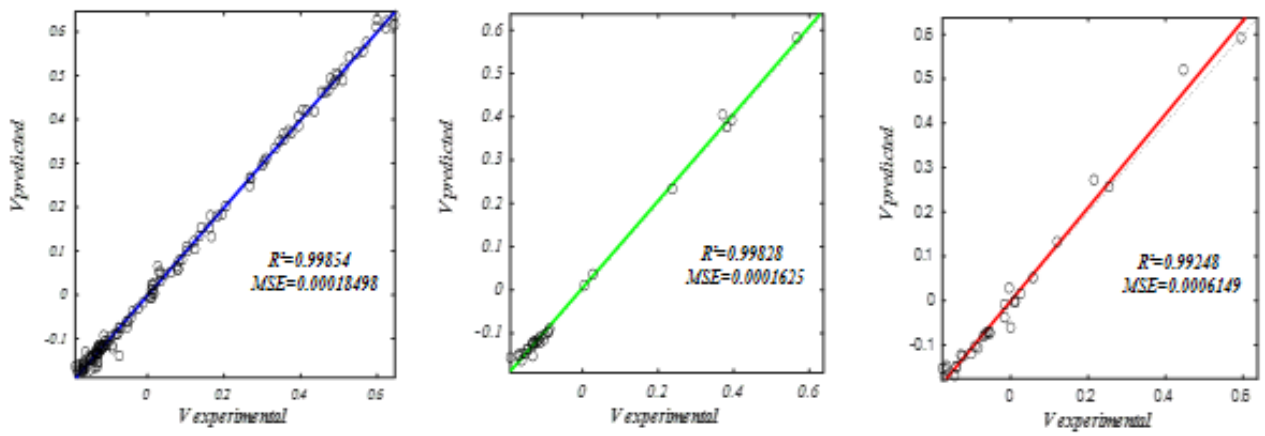

Training set *Validation set* *Testing set*

Figure.III.8: Regression. Radial velocity v in training, validation and testing

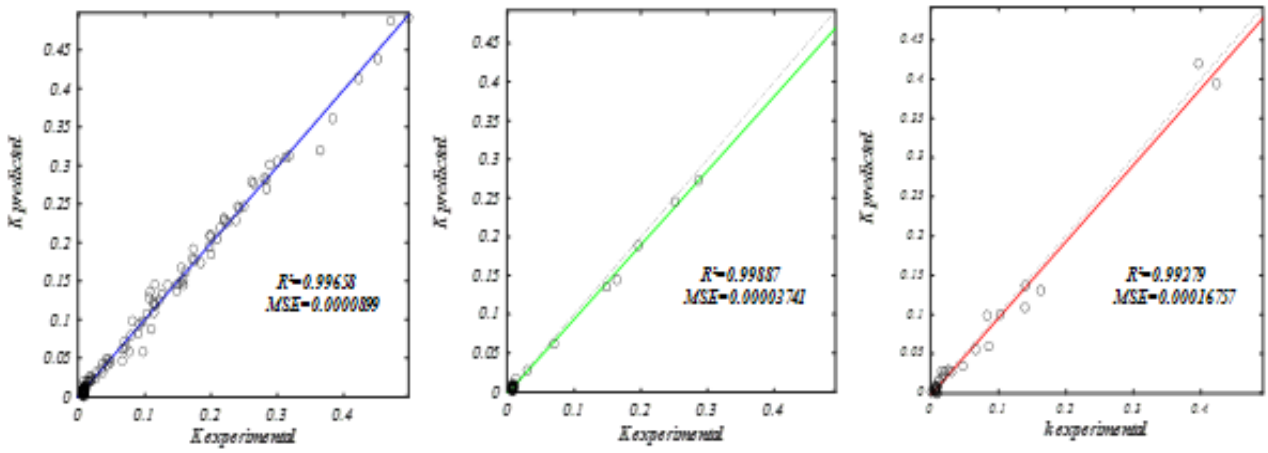

Training set *Validation set* *Testing set*

Figure.III.9: Regression**.** Kinetic energy *k*in training, validation and testing.

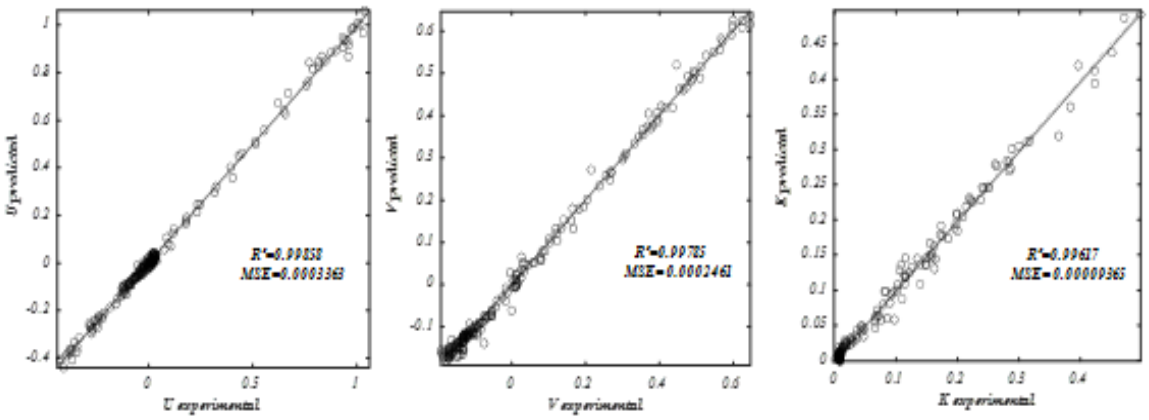

Axial velocity ***Radial velocity*** ***kinetic energy***

Figure.III.10: Regression of all u, v and k**.**

The neural network passes the data several times during the training process and stops when the lowest value is reached for mean square errors MSE. Figure (III.11, III.12, III.13) show the evolution of the mean square errors during the training phase for axial velocity u,

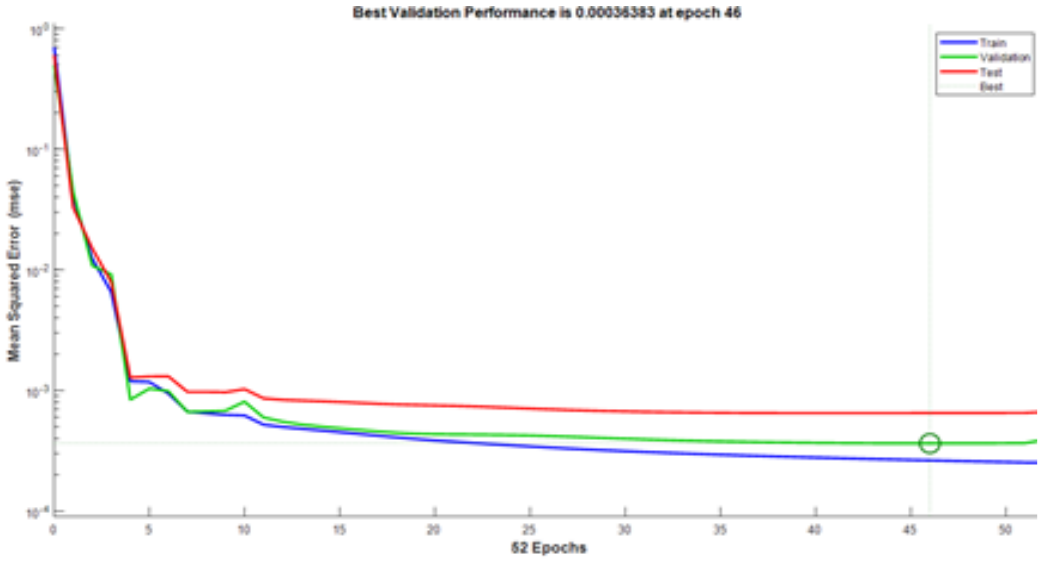

Figure.III.11: The evolution of the mean square errors during the training phase of axial velocity.

radial velocity v, and kinetic energy k, respectively.

We note from Figure III.11 that the best value of the mean square error was in stage 46 of training, which was estimated at 3.6383*10.

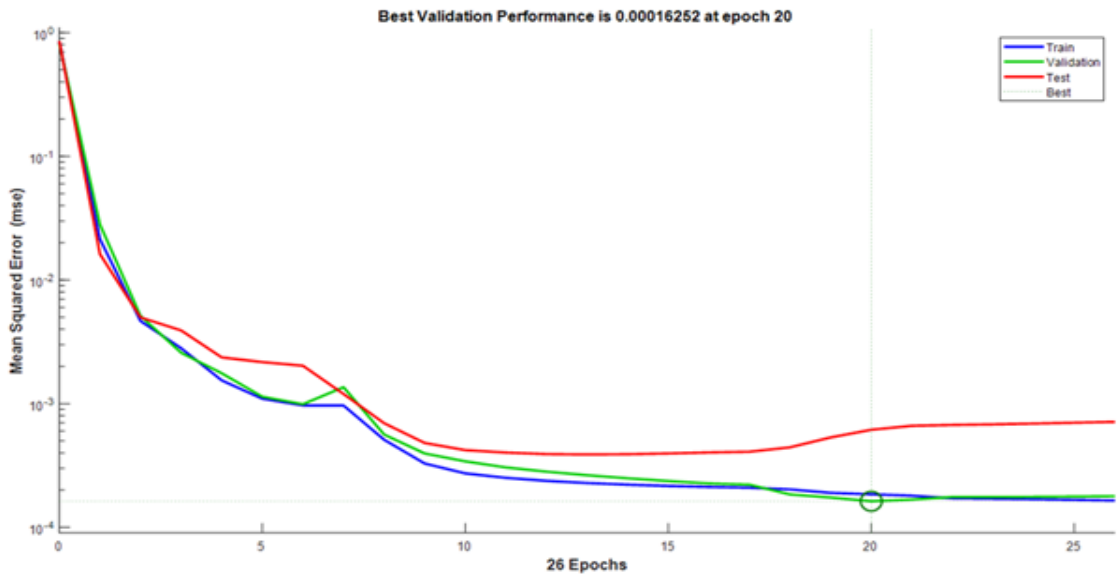

Figure.III.12: The evolution of the mean square errors during the training phase of radial velocity.

It can be seen from Figure III.12 The best validation performance was obtained at epoch 20, with validation plot reaching its minimum MSE value of 0.00016252.

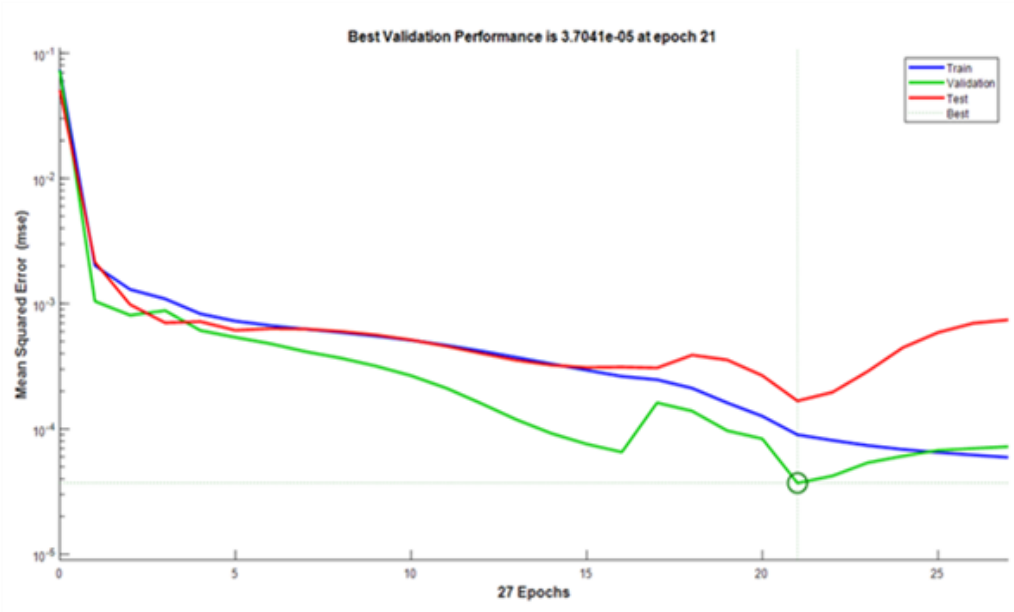

Figure.III.13: The evolution of the mean square errors during the training phase. Of kinetic energy

We note from the Figure III.13 The best validation performance was obtained at epoch 21, with validation plot reaching its minimum MSE value of 0.000037041.

III.4.2.1. Analysis of the results:

-Figure (III.14, III.15, III.16) shows the fit and agreement between the experimental and predicted values for axial velocity, radial velocity, and kinetic energy. With the real values and predicted values agreeing, the relative R error approaches zero, representing the difference between them.

-The introduction of rotor air through two concentric stages provides additional degrees of freedom for controlling the radial distribution of flow and vortex to achieve significantly different combustion characteristics, including flow and mixing patterns, turbulence levels, and different flame stability limits.

- In Figure.III.14, the presence of negative axial velocity values in the vortex flow indicates the existence of reverse flow, or a recirculation zone, along the flow axis. The axial velocity is negative in this region because the axial direction of movement is opposite to the main flow direction. These regions also experience a decrease in flow velocity and an increase in airflow turbulence, which helps mix the reactants. This turbulence is used strategically to improve performance and increase efficiency. Figure. III.16 shows an increase in turbulent kinetic energy in these areas. As we move along the path of the combustion chamber (as shown in Figure.III. 16), the turbulent kinetic energy gradually decreases until it reaches low or negligible levels, because the flame becomes stable at the end of the chamber.

At the vortex core level, the axial velocity is nearly zero. Thus, the presence of zero axial velocity at the vortex core is evidence of proper vortex flow formation. The axial velocity transitions from negative to positive values in the vortex flow when moving from the recirculation zones to areas farther from the vortex core. On the other hand, high positive values indicate a large velocity gradient and high turbulence intensity, which can lead to strong mass and energy exchange.

- As for the radial velocity, it is practically zero at the recirculation zone.

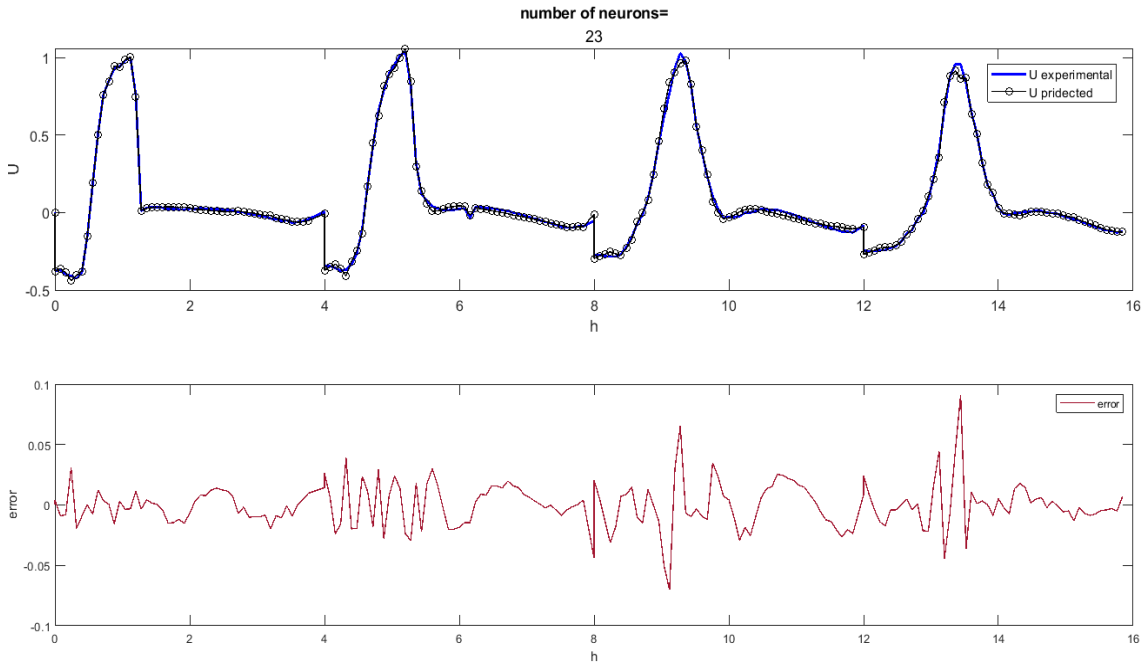

Figure.III.14: Comparison of axial velocity u from prediction and experiment at different locations.

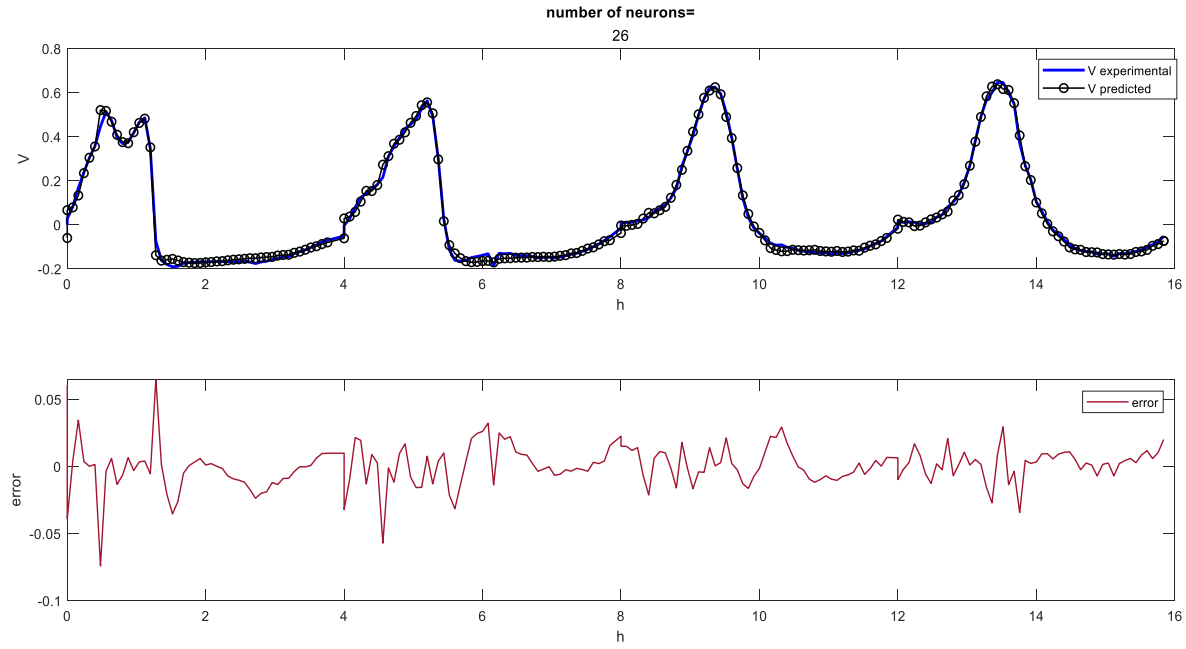

Figure.III.15: Comparison of radial velocity v from prediction and experiment at different locations.

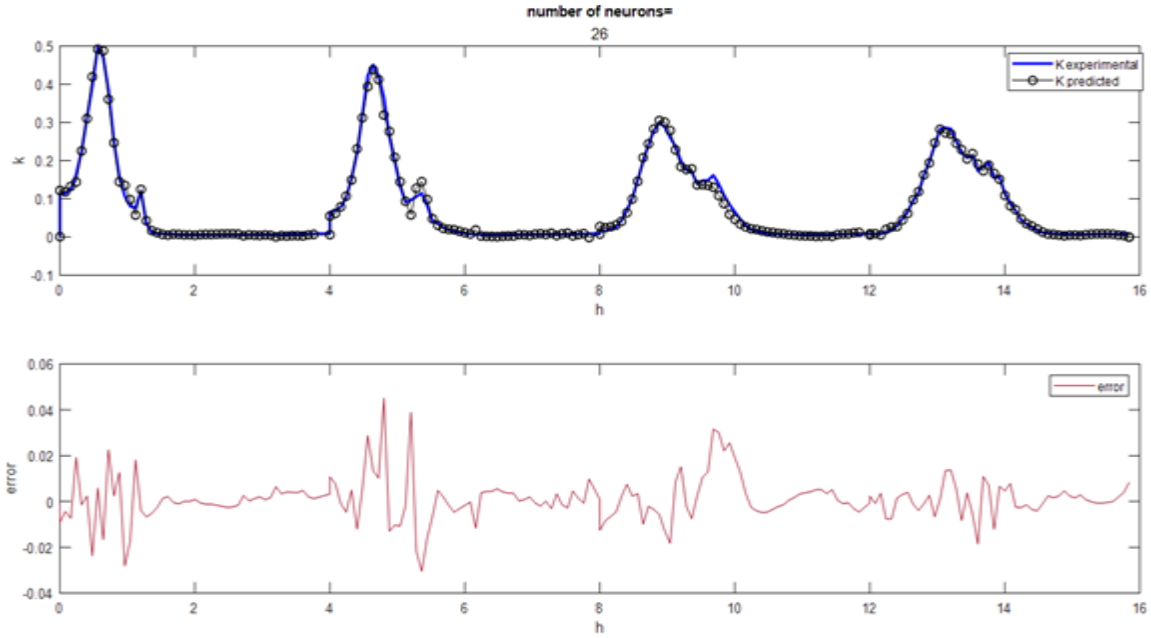

Figure.III.16: Compare kinetic energy k from prediction and experiment at different locations

CONCLUSION:

In this chapter, we analyzed the prediction of swirling flow characteristics, a crucial aspect in industrial systems, utilizing the feed forward backpropagation neural network model. Demonstrating the accuracy and validity of the FFBPN model through curve results, an R^2 value of 0.99, and mean square error (MSE) values, we highlighted the significance of neuron count in achieving accurate outputs. Ultimately, the FFBPN model effectively captures spatial characteristics of swirling flow fields, establishing a strong correlation between input and output parameters. This facilitates accurate predictions of velocity distribution and vortex center positions, aligning well with experimental findings, thus enhancing efficiency in studying and predicting swirling flow phenomena across various flow fields.

GENERAL CONCLUSION

GENERAL CONCLUSION:

During this study, we tried to come up with a model using artificial neural networks that contributes to predicting the characteristics of eddy flow and ensuring its efficiency. Among the most important conclusions we reached through our study of this topic are:

_ Swirl flow is used in industrial systems to improve combustion through excellent mixing of fuel and air and a uniform distribution of temperature, thus returning unburned gases to the flame with a uniform temperature. This shows its importance in economic and industrial systems by improving production efficiency and product quality and reducing environmental impacts from polluting emissions.

_ In the recirculation area, the axial velocity of the flow decreases and the air flow turbulence increases significantly, which forms a reverse flow that leads to negative axial values.

_ The study concluded that the FFBPN artificial neural network model is considered one of the most efficient models that helps in predicting the characteristics of eddy flow on the basis of reaching satisfactory results in calculating the error rate ms e. It has also been found that the accuracy of the output is highly dependent on the number of neurons.

_The model is a feed-forward and feed-back diffusion network capable of accurately predicting the eddy flow field under working conditions given in known data sets, but also has a satisfactory ability to extrapolate the eddy flow field under unknown inlet conditions.

- The advantages of this prediction model, including computational efficiency, adaptability, and rapid response, make it valuable for various applications. Furthermore, it has the potential to extend its capabilities to three-dimensional, multiparameter, and multi-objective flow field predictions. It's important to highlight that this study specifically applies the FFBPNN to a nonreacting swirling flow field. In future endeavors, integrating fuel-air ratio and temperature as inputs into our model can enhance predictions for turbulent reacting swirling flow fields, potentially reducing experimental costs. Additionally, future research will explore feature extraction and prediction in scenarios involving the interaction between combustion species concentration fields and swirling flow fields.

REFERENCES

REFERENCES

[1]. **Syred N**, A review of oscillation mechanisms and the role of the precessing vortex core (PVC) in swirl combustion systems, Progress in Energy and Combustion Science, 32(2), 2006, 93-161.

[2]. **F. Bouras**, Simulation de la combustion turbulente non-prémélangée par le modèle L.E. S ». Thèse de magister, BATNA (2006).

[3]. **Lola Guedot**, Développement de méthodes numériques pour la caractérisation des grandes structures tourbillonnaires dans les brûleurs aéronautiques : application aux systèmes d'injection multi-points. Mécanique des fluides [physics.class-ph]. INSA de Rouen, 2015, Français.

[4]. **R.S. Barlow and J.H. Frank**, Effects of turbulence on species mass fractions in methane/air jet flames. *In Symposium (International) on Combustion*, volume 27, Elsevier, 1998. pages 1087–1095.

[5]. **Sandia**, Experimental data archives.http://www.sandia.gov/TNF/pilotedjet.html

[6]. **T. Poinsot and D. Veynante**, Theoretical and Numerical Combustion, 2011.

[7]. **Panda, J. & McLaughin, D. K**, Experiments on the instabilities of a swirling jet, Phys. Fluids, 6, 263-276 (1994).

[8]. **Beér, J. M. & Chigier**, N. A, Swirling Flow, in Combustion Aerodynamics edited by Krieger, Malabar, Florida, 1972.

[9]. **Leuckel, W. & Fricker**, N., The characteristics of swirl-stabilized natural gas flames. Part I : Different flame types and their relation to flow and mixing pattern, Journal of the Institute of Fuel, 103-112 (1976).

[10]. **M. P. Escudier and J. J. Keller**, Recirculation in swirling flow: a manifestation of vortex breakdown, AIAA Journal, 23, 111-116 (1985).

[11]. **Sheen, H.J. Chen, W.J. Jeng, S. Y. Huang, T. L.**, Correlation of swirl number for a radialtype swirl generator, Experimental Thermal and Fluid Science,12,444-451 (1996).

[12]. **Projet de Physique P6 STPI/P6/2022 –20**, Les brûleurs à swirl, INSTITUT NATIONAL DES SCIENCES APPLIQUEES DE ROUEN.4.

[13]. **Tangirala.V , Chen.R.H and Driscoll.J.F**, Effect of heat release on the recirculation witihn swirl-stabilized flames. Combust.Sci and Tech 1987 Vol 51 pp 75-95.

[14]. **Poireault.B**, Mécanisme de combustion dans un brûleur méthane-air de type swirl (40 kW): influence de l'intensité de la rotation. Thèse de l'université de Poitiers (1997).

[15].**Hill.S.C, Douglas Smoot.L**, Modeling of nitrogen oxides formation and destruction in combustion systems. Progress in energy and combustion science 25 pp417-458 (2000).

[16].**Kamel Guedri,** Numerical Study of the Swirl Effect on a Coaxial Jet Combustor Flame Including Radiative Heat Transfer, Dec 2009.

[17].**P. Schmittel, B. Günther, B. Lenze, W. Leuckel, H.** Bockhorn,Turbulent swirling flames: Experimental investigation of the flow field and formation of nitrogen oxide, *Proceedings of the* Combustion *Institute*, 2000, Pages 303-309.

[18].**Chen.R.H and Driscoll.J.F**, The role of the recirculation vortex in improving fuel-air mixing within swirling flames. Twenty-second symposium international on combustion, pp 531-540 (1988).

[19].**Feikema**, **Chen, Driscoll**, Enhancement of flame blowout limits by the use of swirl ,Comb. and Flame, 1990

[20].**Vauchelles**, Etude de la stabilite et des emissions polluantes des flammes turbulentes de premelange pauvre a haute pression appliquees aux turbines a gaz, INSA de Rouen,2004.

[21].**Susset**, developpement de traitements d'images pour l'etude de la stabilisation de flammes turbulentes non-premelangees generees par des bruleurs industriels modeles, 2002.

[22]. **CHERIFI Mouna,** Simulation Et Caractérisation De L'effet D'un Brûleur A Swirl Sur La Production Des Emissions.Thèse de master. Blida(2020).

[23].**V. Moureau, P. Domingo, L. Vervisch**, (2011), From Large-Eddy Simulation to Direct Numerical Simulation of a lean premixed swirl flame: Filtered laminar flame-PDF modeling, Combustion and Flame, 158(7), pp:1340-1357.

[24].**A. Ateshkadi, V.G. McDonell, G.S. Samuelsen**, Effect of hardware geometry on gas and drop behavior in a radial mixer spray. Twenty-Seventh Symposium International on Combustion 1985, the Combustion Institute, 1985-1992.

[25].**J.C. Broda, S. Seo, R.J. Santoro, G. Shirhattikar, V. Yang**, An experimental study of combustion dynamics of a premixed swirl injector. Twenty-Seventh Symposium International on Combustion 1998, the Combustion Institute, 1985-1992.

[26].**MATHUR, M. L, MACCALLUM, N. R. L.**, Swirling air jets issuing from vane swirls. Part I: free jets. Journal of the Institute of Fuel 1967.

[27].**Schmittel P Et al.** Turbulent swirling flames: Experimental investigation of the flow field and formation of nitrogen oxide. In: 28th Symposium (International) on Combustion. The Combustion Institute. 2000. pp. 303-309.

[28].**ROSE, W. G.**, A swirling round turbulent jet. Journal of Applied Mechanics 1962, 29: pp. 615-625.

[29].**LOPEZ J. M.**, Axsymmetric vortex breakdown. Part1: Confined swirling flow, J. Fluid Mech. 1990, 221: pp. 553-552.

[30].**O Lucca-Negro, T O'Doherty**, Vortex Breakdown: a review. Prog, Energy Combust. Sci. 2001, 27: pp. 431-481.

[31].**SHI, R. X., CHEHROUDI, B.**, Velocity Characteristics of a confined highly turbulent swirling flow near a swirl plate. J. of Fluid Eng. 1994, 16: pp. 685-693.

[32].**Boushaki T, Sautet JC, Labegorre B**, Control of flames by radial jet actuators in oxy-fuel burners. Combustion and Flame. 2009;156:2043-2055.

[33].**P. Palies.** Dynamique et instabilit´es de combustion des flammes swirl´ees. pages 1–288, 2010.

[34].**V. Moureau, P. Domingo, L. Vervisch**, (2011), From Large-Eddy Simulation to Direct Numerical Simulation of a lean premixed swirl flame: Filtered laminar flame-PDF modeling, Combustion and Flame, 158(7), pp:1340-1357.

[35].**W. Leuckel**, Swirl Intensities, Swirl Types and Energy Losses of Different Swirl Generating Devices: Symbols, Definition, Derivations of Formulas-figures, 1967.

[36].**N. Syred et J. M. Beer,** Combustion on Swirling Flows, *Combustion and Flame*23 (1974) 143-181.

[37].**T.C. Claypole et N. Syred,** The effect of swirl burner aerodynamics on NOx formation, *Proc. Combust. Institute* 18 (1981) 81-89.

[38].**R. Rawe et H. Kremer,** Stability limits of natural gas diffusion flames with swirl,*Proc. Combust. Institute* 18 (1981) 667-677.

[39].**R. Hillemanns, B. Lenze et W. Leuckel,** Flame stabilization and turbulent exchange in Strongly natural gas flames, *Proc. Combust. Institute* 21 (1986) 1445-1453.

[40].**D. Feikema, R.H. Chen et J.F. Driscoll,** Enhancement of flame blowout limits bythe use of swirl, *Combustion and Flame* 80 (2) (1990) 183-195.

[41]. **C.K. Chan , K.S. Lau , W.K. Chin , R.K. Cheng**, Freely Propagating Open Premixed Turbulent Flames Stabilized by Swirl, *The Combustion Institute,*

pp. 511-518, (1992).

[42].**Bidat B. et Cheng R.K**., Experimental Study of Premixed Flames in Intense Isotropic Turbulence, Combustion Group, Energy & Environment Diuision, Lawrence Berkeley Laboratory, Berkeley, CA 94720, (1995).

[43].**H.J. *Sheen*, W.J. *Chen*, S.Y. *Jeng*, T.L. *Huang*, Correlation of swirl number for adial-type swirl generator, Experimental Thermal and Fluid Science, May 1996, Pages 444-451.**

[44].**J. Zhang et S. Nieh,** Comprehensive modelling of pulverized coal combustion in a vortex combustor, Fuel 76 (1997) 123–131.

[45].**J. Zhang et S. Nieh,** Swirling, reacting, turbulent gas-particle flow in a vortex combustor, *Powder Technology* 112 (2000) 70–78.

[46].**Ying Huang and Vigor Yang,** Effect of swirl on combustion dynamics in a lean-premixed swirl-stabilized combustor, Proceedings of the Combustion Institute 30 (2005) 1775–1782.

[47].*Khelil* , H. *Naji* , L. *Loukarfi* , G. *Mompean*, Prediction of a high swirled natural gas diffusion flame using a PDF model, Fuel, February 2009, Pages 374-381.

[48]. **I. Yilmaz et al**, (2010): Abdelbaki Mameri, Etude numérique de la combustion turbulente du prémélange Pauvre méthane/air enrichi à l'hydrogène, Université d'Orléans, (2009).

[49]. **B. Sarh, N. Merlo, T. Boushaki, C. Chauveau, S. D. Persis, L. Pillier, I. Gökalp,** (2014), Combustion characteristics of methane–oxygen enhanced air turbulent non-premixed swirling flames, *Experimental Thermal and Fluid Science*, 56, pp: 53-60.

[50].**Sonya Ouali, Mohamed Mhiri, Lotfi Bouzguenda**, A Multidimensional Knowledge Model for Business Process Modeling, Procedia Computer Science, 2016, Pages 654-663.

[51].**A.M. Elbaz, W.L. Roberts**, (2016), Investigation of the effects of quarl and initial conditions on swirling non-premixed methane flames: Flow field, temperature, and species distributions, *Fuel* 169, pp: 120–134.

[52].**M. Boileau, G. Staffelbach, B. Cuenot, T. Poinsot, C. Berat**, (2008), LES of an ignition sequence in a gas turbine engine, *Combust. Flame*, 154, pp: 2-22.

[53].**M. Philip, M. Boileau, R. Vicquelin, E. Riber, T. Schmitt, B. Cuenot, D. Durox, S. Candel**, (2015), Large Eddy Simulations of an annular multiple-injector combustor, Proc. *Combust. Inst*., 35, pp: 3159-3166.

[54].**L. Gang, Z. Yujun, L. Cunxi, J. Xi, C. Qi, X. Gang, M. Yong**, (2017), The Design and Characteristics of a Novel Injector – A Lobed Swirl Injector, Proceedings of

ASME Turbo Expo 2017: Turbomachinery Technical Conference and Exposition, June 26-30,Charlotte, NC, USA

***[55].*Mohamed ELBAYOUMI,** Hydrogen-enriched combustion study at high turbulence and swirl levels inside a gas turbine combustor. Thèse de doctorat électronique, Montréal, École de technologie supérieure,2022.

[56].Junqing *Zhang* , Chunjie *Sui* , Bin *Zhang* , Jun *Li*, Effects of swirl intensity on flame stability and NO emission in swirl-stabilized ammonia/methane combustion, *Applications in Energy and Combustion Science*, June 2023.

[57].**Xinke Shao , Zijian Zhang, Lisong Shi ,Hanli Huang ,Chihyung Wen**, Effects of swirling inflow on the stability and combustion mode of rotating detonations, **Physics of Fluids**, 21FEBRUARY 2024.

[58].**Adel El-Shahat,** Advanced Applications for Artificial Neural Networks: Introductory Chapter: Artificial Neural Networks, 28 February 2018.

[59].**Ajith Abraham,** Artificial Neural Networks, Oklahoma State University, Stillwater, OK, USA,2005.

[60]. **KL. Priddy, PE. Keller,** Artificial neural networks: an introduction, page 2, (2005).

[61]. **D. Graupe,** Principles of artificial neural networks, page 5, (2013).

[62]. **David J. Livingstone,** Artificial Neural Networks Methods and Applications (2009): Overview of Artificial Neural Networks, pp 14–22.

[63].**Kenji Suzuki**, *Artificial Neural Networks -Methodological Advances and Biomedical Applications*, 51000 Rijeka, Croatia: Published by InTechJaneza Trdine. April 2011.

[64].**Lynda AMIMER,** Modélisation et Commande des Systèmes Non Linéaires Fractionnaires par des Réseaux de Neurones Fractionnaires. Thèse de magister, Tizi-Ouzou (2015).

[65].**Abdel-Nasser Sharkawy,** Principle of Neural Network and Its Main Types: Review. Vol. 7 (2020).

[66].**Bekir Karlik and A. Vehbi Olgac,** (1998) Performance Analysis of Various Activation Functions in Generalized MLP Architectures of Neural Networks.

[67].**Hojjat Salehinejad, Sharan Sankar, Joseph Barfett, Errol Colak, and Shahrokh Valaee,** *Recent Advances in Recurrent Neural Networks*, 22 Feb 2018.

[68].**GHODBANE RADHIA,** Résolutions des systèmes linéaires par des réseaux de neurones artificiels, thèse MASTER en Mathématiques, UNIVERSITÈ…MOHAMED KHIDER, BISKRA (Juin 2023).

[69].**P. josh and G. Adam**, Deep Learning a practitioner's approach, Sebastopol: O'Reilly, 2017.

[70].**Nikolaj Buhl,** *Activation Functions in Neural Networks: With 15 examples*, July 25, 2023, from encord: https://encord.com/blog/activation-functions-neural-networks/.

[71].**Siddharth Sharma, Simone Sharma,** (April 2020), *ACTIVATION FUNCTIONS IN NEURAL*, International Journal of Engineering Applied Sciences and Technology, Vol. 4, Issue 12, ISSN No. 2455-2143, Pages 310-316.

[72].**Vadapalli.P,** (2020, 12 20). *7 Types of Neural Networks in Artificial Intelligence*, from upgrad: https://www.upgrad.com/blog/types-of-neural-networks/.

[73].**Md. Saiful Islam, Md. Rafiqul Islam,** Modeling Spammer Behavior: Artificial Neural Network vs.Nai?ve Bayesian Classifier, DOI: 10.5772/16002, April 2011.

[74].**Daniel S, Berman.Anna, L.Buczak ,Jeffrey S. Chavis and Cherita L. Corbett**, *A Survey of Deep Learning Methods for Cyber Security*, Johns Hopkins University Applied Physics Laboratory (JHU/APL1), Laurel, MD 20910, USA (2019).

[75].Salvatore Cuomo1, Vincenzo Schiano Di Cola2, Fabio Giampaolo1, Gianluigi Rozza3,Maziar Raissi4, Francesco Piccialli1, (2022), *Scientific Machine Learning Through Physics–Informed Neural Networks: Where we are and What's Nex.*

[76].**Partice Wira,** Réseaux de neurones artificiels : architectures et applications, Avril 2009.

[77]. B. Li a b, C. Delpha b, D. Diallo a c, A. Migan-Dubois, Application of Artificial Neural Networks to photovoltaic fault detection and diagnosis: A review, March 2021.

[78].**Corisande Lamy** ? Étude de l'utilisation de réseaux de neurones artificiels pour des calculs de haute performance dédiés à la modélisation du transport de sources énergétiques, Modélisation et simulation, Université de Bordeaux, 2022. Français. ffNNT: 2022BORD0308ff. Fftel-03908443f.

[79]. **Maad M. Mijwel, Review Article**: Artificial Neural Networks Advantages and Disadvantages, Mesopotamian journal of Big Data Vol. (2021), 2021, pp. 29–31.

[80]. **Merkle, K, Bu¨chner, H, Zarzalis, N, & Sara**, ON. "Influence of Co and Counter Swirl on Lean Stability Limits of an Airblast Nozzle." Proceedings of the ASME Turbo Expo 2003, collocated with the 2003 International Joint

Power Generation Conference. Volume 2: Turbo Expo 2003. Atlanta, Georgia, USA. June 16–19, 2003. pp. 1-9. ASME. https://doi.org/10.1115/GT2003-38004

[81]. **SHI, R. X., CHEHROUDI, B.,** Velocity Characteristics of a confined highly turbulent swirling flow near a swirl plate. J. of Fluid Eng. 1994, 16: pp. 685-693.

الجمهورية الجزائرية الديمقراطية الشعبية
République Algérienne Démocratique et Populaire
وزارة التعليم العالي والبحث العلمي
Ministère de l'Enseignement Supérieur Et de La Recherche Scientifique
جامعة غرداية
كلية العلوم والتكنولوجيا
قسم الالية والكهروميكانيك
Faculté des sciences et Technologies
Département d'automatique et
d'électromécanique
Université de Ghardaïa

غرداية في : 2024/06/09

إذن بالطباعة (مذكرة ماستر)

بعد الاطلاع على التصحيحات المطلوبة على محتوى المذكرة المنجزة من طرف الطلبة التالية أسماؤهم:

1. الطالب (ة): عطية بشرى..... (ATTIA Bouchra)
2. الطالب (ة): بن عودة هاجر..... (BEN OUDA Hadjer)

تخصص: فيزياء طاقوية وطاقات متجددة

نمنح نحن الأستاذ (ة) :

الاسم واللقب	الرتبة – الجامعة الأصلية	الصفة	الامضاء
Kamel BOUARAOUR	MCA .....Université de Ghardaia	رئيس	
Mohammed ARRIF	MAA .....Université de Ghardaia	ممتحن	
Djemoui LALMI	MCA .....Université de Ghardaia	مؤطر	
Abdessalem Kifouche	MCB .....Université de Ghardaia	مؤطر مساعد	

الإذن بطباعة النسخة النهائية لمذكرة ماستر الموسومة بعنوان

Characterization of a Swirled Flow Using Artificial Neural Networks

جامعة غرداية
قسم الآلية والكهروميكانيك-1
كلية العلوم و التكنولوجيا

إمضاء رئيس القسم
العلمي عبد اللطيف
رئيس قسم الآلية
و الكهروميكانيك